Abstract

Activation of GPR4 by acidosis inhibits tumor cell migration, invasion and metastasis. Reid David Castellone. (Under direction of Dr. Li Yang) Department of Biology. April 2011.

Melanoma and Prostate Cancer are two of the most diagnosed forms of cancer in the United States. The ability to metastasize and colonize in a distant location is one of the most devastating hallmarks of cancer as modes of treatment are severely limited and often inefficient. As cancer accounts for one out of every four deaths in the United States, there is no doubt as to the necessity to develop novel strategies to combat cancer progression. Cancer research has transformed to not only target the actual tumor cells, but also the tumor microenvironment as it is known to play a strong role in tumorigenesis and cancer progression. The defining characteristics of the tumor microenvironment are hypoxia, acidosis and high interstitial fluid pressure, and these characteristics actively select for resistant tumor cells, conferring a progressive phenotype. GPR4, a G-protein coupled receptor, has recently been shown to act as a proton sensor, and as acidosis is a defining characteristic of the tumor microenvironment and GPR4 expression is detected in a wide array of human tissues, it is thought GPR4 may influence tumor cell progression. Therefore, it is the purpose of this study to analyze the biological function acidosis activation of GPR4 has on the ability of tumor cells to acquire a motile and metastatic phenotype. Through a series of cell motility, migration and invasion assays we have determined that GPR4 is activated by acidosis, and that this activation inhibits the motility, migratory and invasive ability of GPR4 overexpressing tumor cells. Furthermore, using a pulmonary melanoma metastasis model, we have shown that GPR4 overexpression significantly decreases the ability for *in vivo* metastasis of tumor cells. To deduce a possible molecular mechanism by which the inhibitory phenotype is

acquired, it was found that GPR4 activation increases the occurrence of actin stress fibers in tumor cells, indicative of upregulation of the $G_{12/13}$-Rho pathway. Furthermore, treatment with CN01, a known cell permeable Rho activator, significantly inhibited both the motility and *in vivo* metastasis of treated tumor cells. In conclusion, it was found that GPR4 is activated by acidosis, and that this activation inhibits the ability for motility, migration and invasion in tumor cells. Furthermore, GPR4 overexpression inhibits the ability for metastasis in a murine model, and it appears that activation of the small GTPase Rho is at least partially involved in the observed motility and metastasis inhibitory phenotypes.

Activation of GPR4 by Acidosis Inhibits Tumor Cell Migration, Invasion and Metastasis

A Dissertation

Presented To the Faculty of the Department of Biology

East Carolina University

In Partial Fulfillment of the Requirements for the Degree

Master of Science in Biology

by:

Reid David Castellone

April, 2011

Activation of GPR4 by Acidosis Inhibits Tumor Cell Migration, Invasion and Metastasis

By:

Reid David Castellone

APPROVED BY:

DIRECTOR OF DISSERTATION:_____
Li Yang, Ph.D.

COMMITTEE MEMBER:_____
Alexandros Georgakilas, Ph.D.

COMMITTEE MEMBER:_____
Maria Ruiz-Echevarria, Ph.D.

COMMITTEE MEMBER:_____
Jean-Luc Scemama, Ph.D

CHAIR OF THE DEPARTMENT OF BIOLOGY:

_____
Jeffrey McKinnon, Ph.D.

DEAN OF THE GRADUATE SCHOOL:

_____
Paul J. Gemperline, Ph.D.

Acknowledgments

I would like to thank the Department of Biology at East Carolina University and the Department of Internal Medicine-Division of Hematology/Oncology at the Brody School of Medicine. These departments provided me the opportunity to advance my love of biology through research, classwork and teaching. The work I have done at East Carolina University has left my prepared and eager for my future academic and professional endeavors.

I am also thankful to Dr. Li Yang and the members of his lab. Dr. Yang has been more than an advisor to me as he has helped me grow and mature in both an academic and professional setting. His mentorship, advice and knowledge have inspired me to reach my full potential and strive for my goals. Furthermore, I would like to thank Nancy Leffler and Lixue Dong for the help, guidance and friendship they have provided me while working in Dr. Yang's lab. Specifically, Nancy contributed towards the MTT data presented in this thesis, while Lixue is responsible for the Claudin-1 western blot data. I could not have completed this work without the help and support of every member of Dr. Yang's lab, and the relationships developed will continue through the future in both an academic and social setting.

I would also like to express my gratitude towards the members of my committee. The support and cooperation my committee exhibited is greatly appreciated.

Finally, I am grateful towards my friends and family for the love and support that they have shown me as I obtain this degree.

TABLE OF CONTENTS

LIST OF FIGURES

Chapter 1: Introduction

Cancer Background and Statistics

Cancer, accounting for one out of every four deaths in the United States, is one of the most pressing health issues under research today [1]. It is a disease generally defined by abnormal and uncontrolled proliferation of cells, often including the unchecked spreading of these tumorigenic cells to distant tissues and organs [2]. Cancer involves dynamic changes in the cell genome that translate into DNA mutations. These mutations produce oncogenes with dominant gain of function, along with a recessive loss of function in tumor suppressor genes [3]. These cancer initiation genetic mutations are caused by internal factors like random mutations of the genome, along with external factors such as tobacco, chemicals and radiation [4].

Behind heart disease, cancer is the most common cause of death in the United States, with more than 1,500 Americans projected to have lost their lives every day in 2010. Furthermore, 2010 saw an estimated 1,529,560 new cancer cases diagnosed [4]. Accounting for 52% of newly diagnosed cancers in men are cancers of the prostate, colorectum and lung and bronchus. In women, cancers of the breast, colorectum, lung and bronchus also account for 52% of newly diagnosed cases [1].

While cancer rates seem astonishing, there is hope for the future as current five year survival trends have seen an increase in survival rates: the survival rate for cancers diagnosed between 1996 and 2003 was 66%, up from 50% in 1975-1977 [4]. Furthermore, there was a 1.3% per year decrease from 2000 to 2006 and a 0.5% per year decrease from 1998 to 2006 in male and female delay-adjusted cancer incidence rates,

respectively [1]. This improvement reflects a progress in the early diagnosis of cancers and an increase in carcinogen awareness, as well as advances in research and treatment. This trend is a direct result of an increased interest in the development of new research strategies, some of which will be discussed further on in this paper.

While every cancer case and type presents unique qualities, there are six general, commonly accepted defining characteristics of cancer. These six characteristics are as follows: self sufficiency in growth signals, insensitivity to growth inhibitory signals, evasion of apoptosis, sustained angiogenesis, tissue invasion and metastasis, and limitless replicative potential [3]. This list takes into account the genetic mutations that result in the expression of dominant cancer promoting oncogenes along with the loss of function of tumor repressor genes. Furthermore, this list is inclusive of a major acquired characteristic of cancer cells that often results in patient death; this characteristic is tissue invasion and metastasis and will be the focus of this paper and my research. While this paper will primarily be focused on tumor cell metastasis and motility, specifically as dictated by precise genetic engineering and interactions with the tumor microenvironment, it is important to remain aware that the invasive phenotype of cancer is due to the combinative effect of the aforementioned six acquired capabilities.

Melanoma and Prostate Cancer

There were an estimated 8,700 deaths due to melanoma in 2010, with a predicted 68,130 new cases of melanoma diagnosed in the same year. These estimates leave melanoma to currently be the fifth and seventh most diagnosed forms of cancer in men and women, respectively. The five year survival rate from 1999-2005 for local melanoma was 91%, however upon metastasizing, this survival rate fell to 15% [4].

Alarmingly, upon diagnosis of the metastatic disease, the median survival period is six to nine months [5]. Unfortunately, the rate of development for novel therapies to combat this disease has not paralleled the increase in occurrence. The primary form of therapy is chemotherapy with alkylating agents, which offers a low response rate of 10% [6]. Furthermore, recent studies have indicated melanoma as a prototype of chemotherapy-resistant tumors, further complicating the development of new combative strategies [7]. However, somatic oncogenic mutations to the signaling transduction molecule v-raf murine sarcoma viral oncogene homolog B1 (BRAF) have been identified in 70% of melanomas and close to one half of analyzed patients with metastatic melanoma, making it the most commonly mutated signal transduction pathway in melanoma [8, 9]. Ultimately, BRAF mutations lead to increased tumor cell proliferation and survival, characteristics that inspire the development of strategies to combat this mutation. Selective BRAF inhibitors have shown very promising results in the clinical setting, with a large percentage (>69%) of patients with BRAF mutated metastatic melanoma showing tumor regression upon administration of varying BRAF inhibitors [9, 10].

With an estimated 217,730 new cases having been diagnosed in 2010, coinciding with 32,050 deaths in the same year, prostate cancer is the most diagnosed and second most deadly form of cancer in men in the United States. Although from 2000 to 2006 there was a 2.4% decrease in incidence rate per year, the incidence rate is still one of the highest and thus an area of concern [4]. As with most cancers, there is a high treatment success rate upon eradication of a localized, primary tumor. However, 70% of patients with advanced prostate cancer see metastasis to the bone, with metastasis severely worsening the patient's prognosis [11].

From the previously described statistical data, the widespread impact of both metastatic melanoma and prostate cancer is astonishing. With melanoma being the seventh most diagnosed form of cancer in women, and melanoma and prostate cancer being the fifth and second most diagnosed forms of cancer, respectively, in men, it is clear how pressing of an issue the development of techniques to combat the spread of these forms of cancer is [4].

Transformations in Cancer Research

Cancer therapy is currently expanding its paradigms from targeting strictly tumor cells to the entire complex of the cancer, inclusive of not only primary tumor cells but also of the microenvironment of said tumor. Traditionally, cancer has been viewed as a disease characterized by mutating and transforming cells that acquire invasiveness and autonomous hyperproliferation, even in the presence of naturally occurring cell death signals. In accordance with this model, therapy has historically centered on targeting the tumor cell itself [12]. As an alternative to traditional tumor cell directed therapy, targeting the tumor microenvironment offers a new area of focus with the possibility of developing many new, radical therapies to the treatment of cancer. This new mode of thinking proposes to treat the tumor as an abnormal organ, inclusive of the molecules, signals and cell types that interact in an interdependent manner. It has been proposed that this recognition of the tumor as a complex organ has potential to produce varying treatments to cancer that are not only more specific, but minimize toxicity and increase the patient's chances of survival. Furthermore, it is thought that targeting multiple components of the tumor microenvironment could in fact overcome escape mechanisms often implemented by the tumor [3, 13].

The Tumor Microenvironment

The aforementioned tumor microenvironment is a broad term inclusive of the supporting structures and cells in the immediate vicinity of the tumor. These cells are normal, non malignant cells embedded within a conglomeration of protein rich extracellular matrix and interstitial fluid. In addition to the stroma, and thus the blood vessels and supportive tissues, the various cell types accounted for in the tumor microenvironment are as follows: endothelial cells and their precursors, pericytes, smooth muscle cells, fibroblasts, carcinoma associated fibroblasts, myofibroblasts, neutrophils, eosinophils, basophils, mast cells, T and B lymphocytes, natural killer cells and antigen presenting cells such as macrophages and dendritic cells [12, 14]. It has been reported that these microenvironment cells exhibit an active role in cancer progression and tumor growth. For example, the connection between inflammation and cancer has long been reported, with Rudolf Virchow reporting the infiltration of leukocytes in tumor tissue in 1863 [15]. It was not deduced until later, however, that the recruitment of leukocytes actually promoted carcinogenesis under some circumstances. Furthermore, inflammatory cells found in the tumor microenvironment, like monocytes and macrophages, contribute to the progression of the cancer by secreting different growth factors that influence tumor cell attributes like motility. Monocytes and macrophages have been reported to secrete vascular endothelial growth factor (VEGF)- A and –C, basic fibroblast growth factor (bFGF), tumor necrosis factor (TNF), hepatocyte growth factor (HGF), epidermal growth factor (EGF) family members, platelet derived growth factor (PDGF), and chemokines like interleukin (IL)-8 [12]. The components of the microenvironment offer an outlet

through which tumors are able to progress through varying stages of angiogenesis and metastasis.

It is seen that tumor microenvironments have three very distinct and unique qualities: high interstitial pressure, hypoxia and low pH. Hypoxia and acidosis result in an increasingly hostile metabolic microenvironment for the cells and tissues located within. Under normal conditions, cells within the body require oxygen and other nutrients for growth and survival. These parameters must be maintained in tissue homeostasis, as facilitated by an exchange of gas, nutrients and metabolites over capillary walls [14]. Tumor cells, however, present a unique case in terms of the previously mentioned homeostasis. Due to the unique, uncontrolled proliferation of cells observed in tumors, the vasculature present in tumor cells is inadequate for maintaining homeostasis in regards to hydrogen ion flux, oxygen diffusion, and lymphatic pressure. It is the interaction, or lack thereof, of tumor cells and tumor vasculature that results in regions of high interstitial fluid pressure (IFP), low oxygen tension, and low extracellular pH [16]. These three conditions are the current focus of much research as they facilitate the metastatic and angiogenic properties characteristic of the majority of invasive tumors. The processes resulting in hypoxia, low pH and high IFP will be discussed below in subsequent sections, as will the tumor cell adaptations that culminate in immunity to the conditionally evoked apoptosis observed in normal, non malignant cells [17]. Furthermore, the increased metastatic and angiogenic potential resulting from said conditions will also be analyzed.

Somatic Evolution of Tumor Cells

As previously stated, cancer cells arise through mutations in the cell's genome, mutations that result in cells with a phenotype characterized by uncontrolled proliferation due to the occurrence of oncogenes with dominant gain of function, along with a recessive loss of function in tumor suppressor genes. These newly formed tumor cells exhibit, in addition to the aforementioned gain or loss of signals, an evasion of apoptosis, limitless replicative potential, sustained angiogenesis and the ability for metastasis [3]. The transformation of these normal cells to benign, pre-malignant, tumor cells, and further to malignant, invasive tumor cells occurs through the process of somatic evolution. This is said due to the analogy between carcinogenesis and Darwinian dynamics as new phenotypes are generated by heritable changes in gene expression and function [17]. These phenotypical changes actively selected for (immunity to hypoxia, low pH etc.) are directly dependent on the cell's interactions with the microenvironmental selection forces. The evolution of these cells coincides with an increase in communication between the microenvironment and tumor cells, as the tumor cells take advantage of the changes in the microenvironment [18]. Therefore, it can be assumed that the arising phenotypes being selected for offer a distinct advantage for the cell in terms of an increase in fitness and sustainability.

Microenvironmental Hypoxia

Due to the large influence of hypoxia in the active selection of tumor cells, along with the subsequent increase in metastatic and angiogenic potential, a detailed description of the conditions that bring about this characteristic must be analyzed. Under normal conditions, cells obtain the majority of their ATP from cellular respiration, inclusive of glycolysis, oxidative decarboxylation of pyruvate, the citric acid cycle and oxidative

phosphorylation. Under these conditions, the pyruvate created in glycolysis is oxidized to acetyl-CoA and CO_2 by the pyruvate dehydrogenase complex. Subsequently, in the presence of oxygen, this acetyl-CoA is transformed into oxaloacetate. These steps, along with oxidative phosphorylation, result in the release of 36 ATP molecules (from one glucose molecule) [19].

Cellular respiration in the presence of oxygen (as previously described) is very efficient. However, as stated, many metastatic tumor cells exist in a hypoxic environment. This hypoxic environment arises due to limits in the oxygen diffusing capability found within tumors [18]. As a normal cell transforms into a pre-malignant cell it exhibits uncontrolled proliferation. Thus, tumor cells are building upon tumor cells in the synthesis of the primary tumor. Concurrent with cellular respiration, these cells are consuming large amounts of oxygen and glucose as they are rapidly dividing. However, the tumor is highly heterogeneous in vascularity [19]. Normal, non-tumorogenic cells transform to tumorigenic cells characterized as hyperproliferative. As the hyperproliferative cells are building on top of each other, and the distance from the cells to the blood vessels is increasing, a diffusion limit is reached at which point the partial pressure of oxygen, pO_2, is zero, and tumor cells must thus rely upon anaerobic glycolysis [18].

The Warburg Effect

As previously noted, tumor cells have evolved to exist in a hypoxic environment. The mechanism for this is described by the Warburg Effect which states that tumors develop a modified sugar metabolism in which a large portion of the blood glucose consumed by the tumor is converted one step beyond pyruvate into lactic acid, even

under normoxic conditions. In other words, even when there is sufficient oxygen in the mitochondria to metabolize the pyruvate in glycolysis to carbon dioxide and oxygen, the glycolytic phenotype is still retained and responsible for the majority of the ATP formed by the cell. The anaerobic glycolysis being carried out by these developing tumor cells is a highly inefficient process, releasing only 2 ATP molecules for every glucose molecule consumed [19-21]. It must also be noted that the glucose diffusion limit is further away from vessels than the oxygen diffusion limit, supporting further the beneficial effects for tumor cells to actively select for glycolysis. Furthermore, this anaerobic glycolysis results in the release of lactic acid into the interstitial space, a process that brings about the low pH found in tumor microenvironments. However, as the Warburg effect dictates, this phenotype is found even in the presence of oxygen, and must thus offer a distinct advantage for processes in the developing tumor cell like proliferation and biomolecule synthesis [18, 20, 22].

The work of Gatenby *et al*. presents a comparison of the rate of glucose consumption between a non invasive breast cancer line, MCF-7, and an invasive breast cancer line, MDA-MB-231, both in hypoxic and normoxic conditions. The highly invasive line shows large amounts of glucose consumption both in normoxic and hypoxic conditions. The non invasive line also exhibits glucose consumption in both conditions, however not nearly to the extent of the highly invasive line. One can therefore observe the constant high rate of glycolysis of invasive cancer cells in aerobic and anaerobic conditions [19].

Microenvironmental Acidosis

The upregulation of anaerobic glycolysis found in tumor cells results in the release of large amounts of lactic acid and carbonic acid into the microenvironment. A trend is observed as the further the replicating cells are from the source of oxygen, the higher the dependency on anaerobic glycolysis, and thus the lower the pH is.

Just as phenotypes that upregulate glycolysis are evolutionarily selected for, so must the phenotypes that are resistant to acid induced toxicity. The exposure of peritumoral normal tissue to an acidic microenvironment brings about toxicity by two different mechanisms. First, necrosis or apoptosis is invoked as the transmembrane hydrogen ion gradient collapses. On top of this, the extracellular matrix also undergoes degradation through the release of proteolytic enzymes [23]. As the tumor cells have evolved to be immune to the acidosis mediated cell death, they are able to survive and proliferate in a low pH environment. On the other hand, normal peritumoral cells are dying, permitting the acidosis resistant tumor cells to invade the available niche [23]. While the role of acidosis in promoting tumor cell invasion and metastasis has been proposed, little is known about whether there are any acidosis-responsive pathways that inhibit cancer metastasis.

G-protein Coupled Receptors

G protein coupled receptors, GPCRs, are transmembrane cell surface receptors, composed of seven transmembrane alpha helices, responsible for transducing numerous extracellular signals into cells, along with playing important roles in the regulation of cell proliferation [24]. For example, GPCRs have a role in regulating neurotransmission, hormone and enzyme release from endocrine and exocrine glands, cardiac and smooth muscle contraction, immune responses and blood pressure regulation [25]. GPCRs are

the largest family of receptors with over 800 members [26]. It has recently been discovered that GPCRs are deregulated in a large number of tumor cells, and it is thus thought that they may be involved in early tumor progression, tumor invasion and metastasis. On the contrary, there have been reports that certain GPCRs, such as OGR1, inhibit tumor cell motility and metastasis by acting as metastasis suppressor genes, and the targeting of such genes offers high therapeutic potential [27]. GPCRs represent the target of 50-60% of all current therapeutic agents for various diseases, resulting in the most prominent family of pharmacological targets [25, 28].

Proton Sensing G-protein Coupled Receptors

It has recently been discovered that the members of a GPCR subfamily, inclusive of GPR4, OGR1, TDAG8 and G2A, are proton sensors in cells through the activity of extracellular histidine residues. OGR1, which shows the most homology to GPR4, has been seen to be inactive at a pH of 7.8, while fully active at a pH of 6.8, the pH observed in most tumor microenvironments [29, 30]. Experiments have confirmed the role of OGR1 in proton sensing, as a ligand independent activation of phosphinositide turnover is observed in cells (Inositol phosphate formation is stimulated by these proton sensing receptors). At a pH of 7.6, IP formation was similar to that of the background, while a pH of 6.8 resulted in significant accumulation of IPs [29]. OGR1 has been seen to be a metastatic suppressor, as OGR1 expression is five times higher in primary tumor cells than metastatic tumor cells [30]. The work of Singh *et al.* illustrates the occurrence of OGR1 fluorescently tagged proteins as observed in tumors. PC3 metastatic tumor cells were injected in the mouse prostate and allowed 45 days to adhere and metastasize. Their results indicated strong metastasis of the control primary prostate tumor cells to the

stomach, diaphragm and spleen, while the OGR1 overexpressing tumor cells were contained to the prostate. Although ORG1 has been demonstrated to function as a proton sensor by several independent studies, Singh *et al*. showed that OGR1 inhibits cell migration in a pH independent manner in their experimental system. It remains to be determined whether their observation can be generalized in other cell systems. Thus, OGR1 expression seems to play a vital role in inhibiting metastatic prostate cancer cell lines in a pH independent manner [30].

GPR4

As previously stated, GPR4 is a proton sensing GPCR sharing 40-50% homology to its family members OGR1, G2A and TDAG8. GPR4 is widely expressed in a variety of tissues inclusive of the ovaries, liver, lung, kidney, lymph nodes, aorta, placenta, prostate, heart and many other tissues [29-31]. Research has implicated that activation of GPR4 leads to cyclic AMP production. Furthermore, the extent of activation is directly correlated to decreases in pH [29]. The production of cAMP, and its downstream effecter protein kinase A, has been shown to inhibit angiogenesis. It is therefore believed the GPR4 plays a role in the inhibition of angiogenesis at an acidic pH. Yang *et al.* have observed a fourfold decrease in microvessel outgrowth of GPR4 expressing wild type aortic rings upon activation in an acidic environment when compared to GPR4 null aortic rings. Furthermore, treatment of the GPR4 null mouse aortic rings with cAMP showed a significant inhibition of angiogenesis. Therefore, it is currently believed that an acidic pH activates GPR4 to negatively regulated microvessel growth, consistent with cAMP production [24]. While this is a conclusive piece of data indicating not only the activation of GPR4 at an acidic pH, but also that this activation

causes a decrease in angiogenesis, more work needs to be carried out to analyze the role of GPR4 activation on tumor cell motility and metastasis. Singh *et al.* reported that GPR4 overexpression has no effect on PC3 prostate cancer cell line migration, although they saw an inhibitory effect upon OGR1 overexpression. Although they report no involvement of GPR4 in tumor cell migration inhibition, future studies need to be broadened so as to incorporate different tumor cell lines and varying pH treatments. As acidosis activation of GPR4 has been reported to initiate different signaling pathways than OGR1, it is possible that the work of Singh *et al*. did not deduce all potential effects of GPR4 activation on tumor cell motility [30].

Proton activation of GPR4, like its family members, regulates cell activity through coupling to G_s, $G_{12/13}$ and $G_{q/11}$ proteins [32]. The G_s protein system leads to adenylate cyclase formation and accumulation of the downstream effecter cAMP. The $G_{12/13}$ signaling pathway leads to the activation of the small GTPase Rho and its downstream effectors ROCK1 and ROCK2. Finally, the $G_{q/11}$ pathway is reported to result in the phospholipase C pathways along with NFAT-driven transcriptional activation [33].

Various reports have indicated GPR4 activation by acidosis is associated with the upregulation of cAMP and Rho levels [29, 33, 34]. Liu *et al.* have suggested that GPR4 does couple to multiple signaling pathways, inclusive of the $G_{12/13}$ pathway, and that this coupling is proton induced. Furthermore, Liu *et al.* highlighted the involvement of multiple histidine residues, specifically H79, H165 and H269, in the coupling of GPR4 to the G_s, $G_{12/13}$ and G_q proteins [34].

Tumor cell metastasis

One of the most devastating aspects of cancer is the ability for cells to metastasize from the primary tumor to distant sites. The incidence of metastasis is directly correlated with an increase in morbidity and mortality as lesions appear in distant organs, severely worsening the patient's prognosis. Surgery and specific types of radiation therapy are widely implemented to control sites of primary cancer formation, however they provide minimal help in controlling cancer cells once metastasis has been initiated. Often, chemotherapy, radiation and hormonal therapy are used in an attempt to retard metastasis, however results are commonly an extension of survival as opposed to complete eradication [21]. Therefore, it is of the utmost importance to develop novel strategies to inhibit the ability of tumor cells to metastasize, inclusive of preventing the acquisition of the invasive phenotype.

Although a complex process, the general steps involved in tumor cell metastasis require cancer cell motility, intravasation, transit in the blood or lymph, extravasation and finally arrest and growth at a new site [35]. Furthermore the final step, arrest and growth of tumor cells at a new site, is an impressively complex feat in itself. Colonization is a term often used to describe the growth of a new tumor, as it requires the culminative organization of tumor cell proliferation, apoptosis and angiogenesis in the newly forming lesion [21].

Tumor Cell Motility

The initial, propagating step of tumor cell metastasis is the ability of said cell to acquire an invasive phenotype through the acquisition of increased motility [36]. This motility arises through alterations in the tumor cell's adherence to other cells and the extracellular matrix, along with the capability of said tumor cells to proteolytically

degrade the surrounding tissue and subsequently propel themselves through the newly created vacant space [21]. Often involved in the acquisition of the motile phenotype is an alteration of cell structure and characteristics in the form of an epithelial-to-mesenchymal transition (EMT). Inclusive in the EMT is the loss of the epithelial cell-cell adhesion molecule E-cadherin in favor of the mesenchymal cell-cell adhesion molecule N-cadherin, with this process being an indication of malignant progression [37]. Tumor cells also respond to secreted signals and proteases from many cells found in the tumor microenvironment, such as endothelial cells, fibroblasts, mesenchymal stem cells, endothelial cells and stromal cells, with the signals from these cells acting as modulators of invasion and migration [38].

The ability for propulsion and movement through open space is mediated through cytoskeleton rearrangement interactions with the cells in the tumor microenvironment. The exact mechanism for this motility, however, is incredibly diverse among different cell types. There are many different types of motility styles, and they are defined by their differences in integrin-mediated cell matrix adhesion, cadherin mediated cell-cell adhesion, cell polarity, extracellular protease activities, and the cytoskeletal arrangement [39].

In general, cell migration in the extra cellular matrix has five hallmark steps. The first of these steps is lamellipodium extension at the leading edge, often requiring leading edge actin polymerization. The second step is the formation of new focal adhesion complexes at the extending edge of the cell via the interaction of integrins with extra cellular matrix ligands. Next comes proteolysis of the extra cellular matrix due to the activity of proteases. The fourth step is the actomyosin contractions due to myosin II

binding to actin filaments. Finally comes tail detachment at the trailing edge, generating a contractile force that coordinates with that of the actomyosin contractions [39, 40].

The aforementioned steps are general characteristics of tumor cell motility. Within differing types of cells, however, exist three primary modes of motility. These three primary modes of motility are single-cell amoeboid, single cell mesenchymal migration, or collective cell migration [41]. Cells undertaking amoeboidal migration have a rounded phenotype void of mature focal adhesions [42]. This form of motility utilizes a propulsive and pushing mechanism as opposed to relying on adherence to the substrate and subsequent pulling [41]. Amoeboidal motility does not require the activity of proteases, as cells are able to squeeze through gaps in the extracellular matrix as opposed to degrading it [43]. In opposition to amoeboidal motility is mesenchymal motility, which requires high levels of attachment via focal adhesion complexes and cytoskeletal contractility [41]. Cells undergoing mesenchymal motility are characterized by fibroblast like, elongated cell morphology. Furthermore, these cells have established polarity and their invasion is dependent upon proteolysis degradation of the ECM [39]. Finally, collective cell motility involves the migration of sheets, strands and clusters of cells that maintain cell-cell junctions. Parts of the pathway resulting in collective cell motility are similar to that resulting in mesenchymal motility, however the exact mechanisms of this form of motility have much to be deduced [39, 41].

Role of the $G_{12/13}$-protein/Rho Signaling Pathway in Tumor Cell Motility

There is no doubt as to the necessity of cytoskeletal rearrangement in cell motility and metastasis. It is thought that the activation of Rho and the subsequent activation of Rho kinases (ROCK1 and ROCK2) is specifically involved in cell contractility and

cytoskeletal rearrangement. This suggests a possible involvement of the Rho/Rho kinase pathway in different aspects of metastasis, specifically cell migration, invasion, cell-cell adhesion and actomyosin contraction [34]. While many reports have indicated the involvement of Rho in cell motility [44], cell movement is a very complex procedure with many factors contributing towards its progression or inhibition. The process of cancer cell migration is a culmination of the coordination between cytoplasmic membrane protrusions in leading lamellipodia, new adhesions at the leading edge, new organization and construction of filaments throughout the cell body, and finally detachment at the tailing edge. The Rho family of GTPases (Rho, Rac and Cdc42) plays a role in cell motility with Rac and Cdc42 regulating lamellipodia and filopodia formation and direction of motility, Rho assisting in the formation and maintenance of focal adhesions and the formation of actin stress fibers, and ROCK contributing towards myosin light chain phosphorylation and subsequent actomyosin based contractility [36, 39, 44].

While it is clear that the Rho family of GTPases contributes, in many areas, to cell motility, a fine equilibrium must be obtained to ensure this movement. The motility of mesenchymal like cells that have an elongated, fibroblast like phenotype proves to be a balancing act of sorts. It is reported that the activity of RhoA and its effector ROCK needs to be reduced to extend protrusions at the leading edge of the cell, a crucial aspect for cell motility [45, 46]. It is therefore thought that inhibiting these proteins in mesenchymal like cells will return minimal effects [39]. The work of Vial *et al.* found that elevated levels of activated Rho inhibited colon carcinoma cell motility, with this phenotype being attributed to an increase in stress fiber formation and focal adhesions,

which subsequently inhibits protrusions and cell motility [36]. Therefore it is evident that a tight control of Rho activity is crucial to balance cell contraction and adhesion.

As previously mentioned, one of the prominent pathways activated by proton induced activation of GPR4 is the $G_{12/13}$ signaling pathway, as indicated by an upregulation in activities of a Rho pathway reporter construct [33, 34]. This pathway has been reported to be activated by other G-protein coupled receptors, inclusive of OGR1 and $S1P_2$ [33, 47]. Furthermore, Takashima *et al.* reported that $S1P_2$ induced activation of Rho inhibited migration in vascular smooth muscle cells [47, 48]. These reports coincide with other findings that Rho is upregulated in tumor cell motility inhibition as Vial *et al.* demonstrated a necessary downregulation of Rho-GTP levels in the promotion of colon carcinoma cell migration [36]. There is clearly a direct link between an upregulation of the $G_{12/13}$/Rho pathway and acidosis activation of GPR4, however the effects of this activation on tumor cell migration and motility have yet to be deduced.

Chapter 2: Materials and Methods

The B16F10 mouse melanoma, TRAMP-C1 mouse prostate cancer, NIH3T3 mouse embryonic fibroblast cell lines, and primary HUVEC human umbilical vein endothelial cells were used for these experiments. All mouse cell lines express residual levels of endogenous GPR4 (mGPR4). B16F10, TRAMP-C1, and NIH3T3 cells were originally from American Type Culture Collection (ATCC), and HUVEC cells were obtained from Cambrex (now a part of Lonza). Dr. Li Yang from the Department of Internal Medicine/Division of Hematology/Oncology at the East Carolina University Brody School of Medicine provided the cancer cell lines along with all the materials and funding for these experiments.

Dr. Yang was also responsible for the design and development of the cell lines used. The open reading frame of human GPR4 (GenBank accession number NM 005282) was amplified from human cDNA samples by polymerase chain reaction (PCR) with the high-fidelity pfu-turbo DNA polymerase (Stratagene, La Jolla, CA). The PCR primer pair was: sense strand 5'- ATAAGAATGCGGCCGCACCATGGGCAACCACACGTG -3' and antisense strand 5'- ATAAGAATGCGGCCGCTCATTGTGCTGGCGGCAGCAT -3'. A NotI restriction enzyme cut site was engineered at each end of the PCR fragment and the Kozak consensus sequence was added before the translation start codon ATG to achieve efficient translation. The amplified PCR fragment was digested with the NotI restriction enzyme and cloned into the retroviral expression vector MSCV-IRES-GFP as previously described [49]. The resulted construct, named MSCV-huGPR4-IRES-GFP, was sequenced from both strands to verify no mutations existing in the coding region. To make stable cell lines, retroviral transduction was performed as previously described

[49]. Briefly, the MSCV-huGPR4-IRES-GFP or MSCV-IRES-GFP retroviral vector was co-transfected with the pCL10A-1 packaging vector into HEK 293T cells to produce retroviral particles, which were used to transduce B16F10 and TRAMP-C1 cells to make stable cell lines. As the retroviral vector expresses the GFP marker, cells with stable exogenous gene expression were selected by the GFP signal using a fluorescence activated cell sorter (FACS).

Cell Culture

B16F10 and NIH3T3 cells were both maintained in Dulbecco's Modified Eagle's Medium (DMEM) (Gibco) supplemented with 10% Fetal Bovine Serum (FBS) (Invitrogen). TRAMP-C1 cells were maintained in DMEM with 5% FBS, 5% Nu-Serum IV (Invitrogen), 5ug/mL Insulin-Transferrin-Selenium-X (Gibco), and 0.01nmol/L dihydrotestosterone (Gibco). HUVEC cells were grown in Endothelial Cell Growth Medium-2 (EGM-2) (Lonza). All cells were cultured in a tissue culture incubator at 37^{o}C with 5% CO_2. 0.25% Trypsin-EDTA (Gibco) was used for cell detachment. Dulbecco's Phosphate Buffered Solution 1x (dPBS) (Gibco) was used for cell washing. For experiments involving pH, 7.5mM HEPES, 7.5mM EPPS [*N*-(2-hydroxyethyl)-piperazine-*N*'-3-propanesulfonic acid], and 7.5mM MES [2-(4-morpholino) ethanesulfonic acid] (HEM) was used in conjunction with 5N NaOH and 5N HCl to buffer the appropriate media to the desired pH. All cells were grown on 60mm or 100mm culture plates (Corning). All cells used in the following experiments were passed for 2-10 generations and care was taken to prevent growth greater than 90% confluency.

RT-PCR

RNA extraction was performed as recommended by the RNeasy Plus Mini Kit (Qiagen). All solutions and reagents were obtained from the kit. Cells were grown to less than 90% confluency on a 10cm plate and lysed with 600μL of Buffer Rlt Plus. Lysate was collected and passed 5 times through a 20 gauge needle fitted to an RNAse free syringe. Lysate was then transferred through a gDNA eliminator spin column placed in a 2mL collection tube. The column was then spun for 30 seconds at greater than 10,000 rpm, at which point the column discarded and the flow through saved. 600μL of 70% ethanol was then added to the flow through and mixed well. The sample was then transferred to an RNeasy spin column placed within a 2mL collection tube. The tube was then spun for 15 seconds at 10,000 rpm. The flow through was then discarded and 700μL of Buffer RPE was added to the RNeasy spin column and centrifuged for 15 seconds at 10,000 rpm. The flow through was once again discarded and 500μL of Buffer RPE added to the RNeasy spin column. The column was centrifuged for 2 minutes at 10,000 rpm. The column was removed from the collection tube, placed in a new 2mL collection tube, and centrifuged for 1 minute at 10,000 rpm. After placing the column in a new 1.5mL collection tube, 50μL of RNase-free water was added to the spin column membrane and centrifuged for 1 minutes at 10,000 rpm to elute the RNA.

To convert the RNA to cDNA, 1μL of Random Primer was added to 5μg RNA and the volume was adjusted to 12μL with sterile, Rnase free distilled water. Next, the mixture was heated to 70°C for 10 minutes and chilled on ice. The contents of the tube were collected by brief centrifugation, and 4μL of 5X First Strand Buffer (250mM Tris-Cl, pH 8.3, 375mM KCl, 15mM $MgCl_2$), 2μL of 0.1M DTT, and 1μL 10mM dNTP mix (10mM each dATP, dGTP, dCTP, and dTTP at neutral pH). The contents were mixed

and incubated at room temperature for 12 minutes. 1μL of SUPERSCRIPT II was then added and gently pipette up and down. The mixture was then incubated for 50 minutes at 42°C. The reaction was inactivated by heating at 70°C for 15 minutes, leaving the cDNA product.

The following reagents (Invitrogen) and volumes were used per cDNA sample for the PCR reaction:

- 2μL cDNA
- 1μL primers (10μM each)
- 2.5μL 10x Buffer
- 0.75μL 50mM $MgCl_2$
- 0.5μL 10mM dNTPs
- 18μL H_2O
- 0.25μL Taq (5 U/ μL)

The PCR primer pair used for huGPR4 amplification was: sense strand 5'-ACCTCTATCGGGTGTTCGTG -3' and antisense strand 5'-TGCCTGCAAAGGGTCGCTAC -3'. For mGPR4 activation, the primer pair used was sense strand 5'- CAAGACCCACTTGGACCACA -3' and antisense strand 5'-TGTCCTGGGCCTCCTTTCTA -3'. 35 Cycles were performed at an annealing temperature of 58°C.

For quantification, Gel Pro Analyzer software (Media Cybernetics) was used. The optical density was determined for each sample and normalized to the β-Actin internal control. The fold ratio of amplification was then determined in comparison to the least amplified signal (mGPR4 of TRAMP-C1/GPR4 cells).

Transwell Migration and Invasion Assays

B16F10 and TRAMP-C1 cells were grown to 50-75% confluency on 10cm cell culture plates. The cells were then washed in dPBS, trypsinized, stained with Trypan blue to ensure viability, and counted using a hemacytometer. $1x10^5$ tumor cells were resuspended in 100μL of pH buffered DMEM with 0.1% BSA (Sigma) (migration media), and applied to the top of a transwell membrane with 8μm pores. For a chemoattractant, NIH3T3 cells were grown for three days, the growth media collected, pH buffered, and 600μL applied to the bottom of each transwell. Following migration, cells were fixed for 10 minutes with 70% ethanol and allowed to dry, then stained for 10 minutes with 0.2% Crystal Violet (Sigma) and three different fields counted using a 10x objective under an inverted microscope.

To resemble invasion through the extra cellular matrix (ECM), 50μL of an ice cold 1:2 dilution of matrigel:ice-cold water, thawed on ice, was applied evenly and void of bubbles to the top of each transwell and allowed to incubate for 1 hour prior to introducing $1x10^5$ B16F10 or TRAMP-C1 cells resuspended in 100μL of pH buffered migration media. NIH3T3 3-day pH buffered conditioned media was then applied to the bottom of the transwell and cells allowed to invade. Following invasion, the matrigel and migration media was removed, and the cells fixed, stained, and counted as previously described.

To resemble invasion through an endothelial cell monolayer, $1x10^5$ HUVEC cells were added to the top of each transwell, with EGM-2 added to the lower well, and allowed to grow to confluency for 24 hours, at which point B16F10 or TRAMP-C1 cells were introduced and allowed to invade as previously described. Prior to their detachment

and introduction to the transwell, the tumor cells were stained for 30 minutes using 2mM cell tracker orange (Invitrogen) so as to distinguish invading tumor cells from endothelial cells. Invaded tumor cells were counted using a fluorescent microscope.

Wound Closure Assay

$2.5x10^5$ B16F10 or TRAMP-C1 tumor cells were plated in individual wells of a 24 well plate and allowed 24 hours to attach and grow to confluency. A 10μL pipette tip was then used to create a wound through the center of the confluent cell layer. Cells were then treated with 1mL of the appropriate pH buffered growth media, either DMEM + 10% FBS for B16F10 cells or TRAMP media for TRAMP-C1 cells. Photos were taken of the wound periodically throughout the assay. To quantify the data, the size of the wound was determined at the beginning of the assay and compared to the size of the wound upon assay commencement. This analysis gave the distance (μm) that the tumor cells were able to close the wound.

For wound closure assays involving the treatment with the known cell permeable Rho activator CN01 (Cytoskeleton, Inc.), 0.5unit/mL CN01 or 2.5μL/mL DMSO (CN01 solvent) was added to the appropriate pH buffered growth media.

Rhodamine Phalloidin Staining of Actin Stress Fibers

B16F10 cells were grown to less than 50% confluency on an 8-chambered slide (Lab-Tek), at which point they were serum starved by treating with DMEM + 1% FBS for one day and DMEM + 0% FBS for two days. Tumor cells were then treated with pH buffered DMEM or DMEM + 0.5unit/mL CN01. After treatment, the cells were washed with 37ºC dPBS and fixed with a fixative solution consisting of 10% Formaldehyde (Fischer) and 90% dPBS. Next, dPBS was used to wash the cells and they were

permealized with a permealization buffer consisting of 5% Triton X-100 (Bio Rad) and 95% dPBS. Cells were then stained with 100nM Rhodamine Phalloidin (Cytoskeleton) and incubated in the dark for 30 minutes. Mounting media with DAPI (Vector) was then applied and the actin fibers observed using a fluorescent microscope.

Extra Cellular Matrix Degradation Assay

To analyze degradation of the extra cellular matrix, 0.2% gelatin (Sigma) was conjugated with Alexa Fluor 555 (Molecular Probes). Alexa Fluor 555 is known to have a succinimidyl ester moiety that reacts with primary amines to form protein-dye conjugates. Protein-dye conjugation was performed as dictated in the Alexa Fluor 555 Protein Labeling Kit and is summarized below. 50μL of a 1 M solution of the provided sodium bicarbonate was added to 0.5mL of 2mg/mL gelatin. This protein solution was then added to the provided vial of Alexa Fluor 555 dye and the dye dissolved completely for 1 hour at room temperature. Next, the provided purification resin was packed into the provided column and the gelatin-dye solution added to the top. The provided elution buffer was used to elute the labeled protein through the column. A UV lamp was used to observe the elution of the labeled protein and the first fluorescent band collected. The sample collected was the protein-dye conjugate.

To confirm conjugate of the gelatin with the Alexa Fluor 555 dye, gel electrophoresis was run on the gelatin protein and gelatin-Alexa Fluor 555 conjugate. The gel was washed three times for 15 minutes with 15mL of deionized water. 20mL of GelCode Blue Stain Reagent (Thermo Scientific) was used to stain the gel for 1 hour. The stained gel was then washed for 1 hour with ultrapure water, with the water being changed periodically. Samples were observed under white light and UV light.

The confirmed gelatin-Alexa Fluor 555 conjugate was then applied to the top of 18mm cell culture coverslips in the following manner. Coverslips were autoclaved and placed in individual wells of a 12 well cell culture plate, at which point each coverslip was treated with 1mL of a 0.5μg/mL solution of Poly-L-Lysine (Sigma) for 20 minutes. Slips were then washed three times with 1mL of dPBS containing calcium chloride and magnesium chloride (Sigma). After the third wash, coverslips were coated with 1mL of 0.5% glutaraldehyde (Electron Microscopy Sciences) and incubated for 15 minutes at room temperature. Coverslips were again washed three times with the aforementioned dPBS, however it was not aspirated after the third wash. The Alexa Fluor 555-gelatin conjugate was mixed at an 1:8 ratio with 0.2% gelatin and placed in a 37°C water bath. Parafilm was pressed to the workbench to prevent sliding and 80uL of the 1:8 Alexa Fluor 555-gelatin:0.2% gelatin mixture deposited on the parafilm. Coverslips were lifted with forceps and a needle and inverted on the drops of gelatin matrix. Coverslips were allowed 10 minutes to incubate at room temperature at which point they were stored at 4°C.

$2x10^4$ B16F10 cells, resuspended at $2x10^4$ cells/mL, were introduced to the top of each coverslip. Cells were allowed 8 hours to attach at which point they were treated with pH buffered growth media. After 28 hours degradation was observed via fluorescent microscopy. Analysis was performed by counting the cells per area under the bright field and comparing this to the number of degraded regions corresponding to cells. Furthermore, the area of degradation was analyzed using ImageJ (NIH) software. Photos were also taken at the 28 hour mark.

Claudin-1 Western Blot Analysis

HUVEC cells transduced with the MSCV-IRES-GFP vector were grown in EGM-2/HEM medium at pH 8.4 until 90% confluent. Cells were then treated with EGM-2/HEM media at pH 8.4, 7.4, or 6.4 for 15 hours, and lysed in ice-cold RIPA lysis buffer (50mM Tris-HCl, pH 7.4, 150mM NaCl, 1% Triton X-100, 0.25% Na-deoxycholate, 1mM EDTA, 1mM phenylmethylsulfonyl fluoride, 1mM Na_3VO_4, 1mM NaF, 5% protease cocktail inhibitor) (Sigma) for 15 minutes at 4^{o}C. The cell lysates were clarified by centrifugation at 14,000 × g for 15 minutes at 4^{o}C. Protein concentration of the supernatant was determined by the Bradford protein assay (Bio-Rad, Hercules, CA). 15-20µg cell lysates were separated on a 4-12% Bis-Tris gel (Invitrogen). The expression of Claudin-1 was analyzed by Western blotting with the rabbit polyclonal anti- Claudin-1 antibody (Invitrogen), followed by the incubation with the horseradish peroxidase (HRP)-conjugated goat anti-rabbit IgG secondary antibody (Santa Cruz Biotechnology). Chemiluminescence signals were detected using the Amersham ECL Advance Western blotting detection kit (GE Healthcare).

Care of Laboratory Animals

Male and female C57BL/6 mice, 6-8 weeks old, were purchased from The Jackson Laboratory (Bar Harbor, Maine) and bred at the ECU animal facility. All mice were cared for and housed according to current IACUC regulations. Mice were kept on a 12 hour light/dark cycle in a climate controlled room at the ECU Brody School of Medicine Department of Comparative Medicine. All female mice used in the current studies were C57BL/6 wildtype.

Pulmonary Melanoma Metastasis

To observe the *in vivo* metastatic ability of B16F10 melanoma cells, a tail vein assay was performed to observe pulmonary metastasis. B16F10 cells were grown to 50-75% confluency on 10cm cell culture plates, trypsinized, and washed twice with ice cold dPBS, at which point the cells were counted using a hemacytometer. Tumor cells were then resuspended at a concentration of $4x10^5$ cells/mL in ice cold dPBS. 8-14 week old C57BL/6 female mice were place in a mouse holder and their tails submerged in warm distilled water to dilate the blood vessels. $2x10^5$ cells, resuspended in 0.5mL ice cold dPBS, were injected into the lateral tail vein. Intravenous tumor injections allow for the transport of cells throughout the vasculature and offer a model for the eventual arrest, extravasation and subsequent colonization of tumor cells in the lung complexes. This procedure is commonly used for the evaluation of metastasis in a murine model [50]. Mice were observed daily for morbidity and general health until being euthanized by CO_2 asphyxiation 16 days post injection. The lungs were then dissected and fixed in Fekete's Solution (100mL 70% ethanol, 10mL formalin, and 5mL acetic acid) and the tumor nodes counted using a dissecting microscope.

For tail vein injections involving treatment with the known Rho activator CN01, tumor cells were pretreated for two hours with 0.5unit/mL CN01 or 2.5μL/mL DMSO in serum free DMEM. The remaining steps are identical as above.

Subcutaneous Melanoma Injection

This assay allows for the visualization of a subcutaneous primary tumor in a precise, predetermined area, and is widely used as an accepted model for the evaluation of primary tumor growth [50]. B16F10 cells were grown to 50-75% confluence on 10cm cell culture plates. Cells were then washed with ice-cold dPBS, trypsinized, resuspended

twice in ice-cold dPBS, counted, and resuspended at $1x10^6$ cells/mL in ice-cold dPBS. Mice were then anesthetized with 0.05mL/10g body weight of a 9:1 mixture of Ketamine to Xylazine (provided by the ECU Department of Comparative Medicine) and shaved using an electric razor. $2x10^5$ cells were then injected subcutaneously into the right hip flank of the mouse and a primary tumor allowed to form. Primary tumor measurements were taken every three days and mice examined for morbidity and general health. Mice were euthanized by CO_2 asphyxiation after 14 days, at which point the tumors were dissected, fixed, and weighed. For subcutaneous melanoma injections involving the known Rho activator CN01, tumor cells were pretreated for two hours with 0.5unit/mL CN01 or 2.5μL/mL DMSO in serum free DMEM. The remaining steps are identical as above.

MTT Assay

B16F10/Vector and B16F10/GPR4 cells were plated at $5x10^3$ cells/well in a 96 well plate and allowed 2 hours to attach, at which point cells were treated with pH buffered growth media. 15μL of MTT Dye (Promega) was then added to each wells and allowed 2 hours to incubate. After incubation, 100μL of stop solution (Promega) was then administered to each well and the precipitate thoroughly resuspended. The plate was then read at 570nm and 650nm using a spectrophotometer to determine the MTT ratio. Plates were read at the same time for three consecutive days, with care being taken to refresh the pH buffered growth media.

Statistical Analysis

Statistical analysis was carried out using Prism software. Non-paired t-tests were performed with *$P<0.05$, **$P<0.01$, and ***$P<0.001$.

Chapter 3: Results

Confirmation of huGPR4 Overexpression in B16F10 and TRAMP-C1 Cells

B16F10 mouse melanoma and TRAMP-C1 mouse prostate cancer cell lines were stably transduced with human GPR4 (huGPR4) to investigate its function in the mentioned cancer cell lines. As illustrated in Figure 1, RT-PCR confirmed that the huGPR4 transcript is only expressed in the B16F10/MSCV-huGPR4-IRES-GFP (B16F10/GPR4) and TRAMP-C1/MSCV-huGPR4-IRES-GFP (TRAMP-C1/GPR4) cell lines, and that the B16F10/MSCV-IRES-GFP (B16F10/Vector) and TRAMP-C1/MSCV-IRES-GFP (TRAMP-C1/Vector) cell lines contain only the empty vector. Furthermore, as expected, there were equal, low levels of endogenous mouse GPR4 (mGPR4) amplification in all four cell types.

GPR4 Activation in an Acidic Environment Inhibits Tumor Cell Motility

A wound closure assay was performed to analyze the effect of GPR4 overexpression and subsequent activation on tumor cell migration. After creating a wound in a confluent monolayer of tumor cells, the cells were then treated with pH buffered growth media and their ability to close the wound observed. This data established that GPR4 is activated at an acidic pH, and that activation of GPR4 results in an alteration of the motility phenotype in B16F10 and TRAMP-C1 tumor cells. Tumor cells that overexpressed the vector showed only a slight inhibition of motility at an acidic pH, which could be attributed to the expression of residual levels of mGPR4 or other currently unknown reasons. However, upon full activation of overexpressed GPR4 at a pH of 6.4, there was a significant ($p<0.05$) inhibition of the ability for wound closure when compared to vector cells at pH 6.4 and GPR4 overexpressing cells at pH 7.9

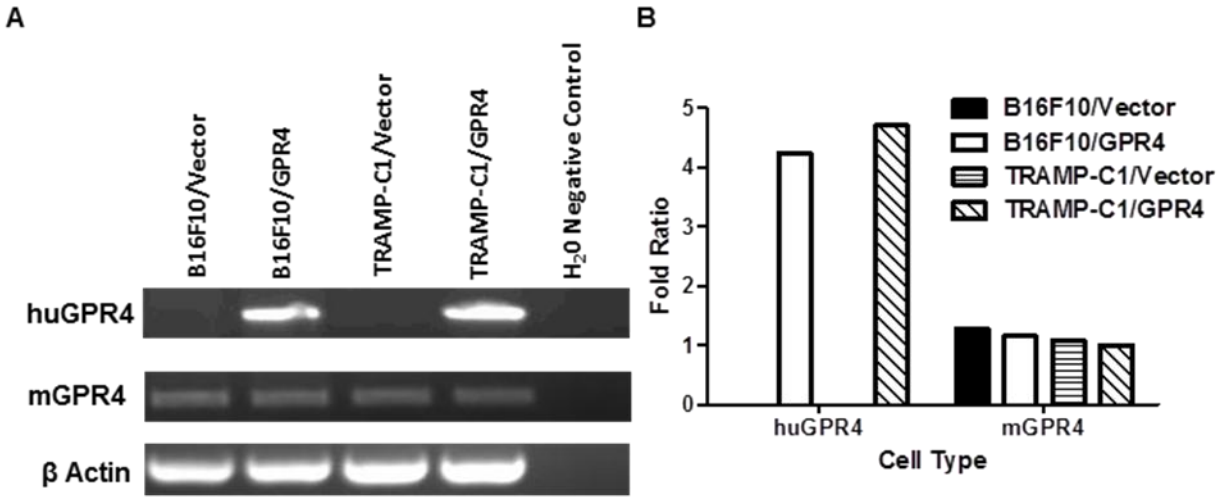

Figure 1. RT-PCR Amplification of huGPR4 and mGPR4 in B16F10 and TRAMP-C1 Cells. (A) Images of RT-PCR amplification of huGPR4, mGPR4 and β-Actin. RT-PCR was performed on RNAs isolated from B16F10/Vector, B16F10/GPR4, TRAMP-C1/Vector and TRAMP-C1/GPR4 cells. Primers were designed to amplify either the huGPR4-IRES sequence or mGPR4. β Actin was used as an internal control and the water used during the assay as a negative control. (B) Quantification of RT-PCR amplification of huGPR4, mGPR4 and β-Actin. The optical density was measured for each sample and normalized to the β-Actin internal control. A fold ratio was then determined for quantification of the amplification.

(Figure 2). This phenotype was observed for both B16F10/GPR4 and TRAMP-C1/GPR4 cells and implies an inhibition of cell motility upon complete activation of GPR4. Figure 2 offers both a qualitative (2A) and quantitative (2B, 2C) representation of this data.

GPR4 Activation in an Acidic Environment Inhibits Tumor Cell Directional Migration

After determining that GPR4 was activated at an acidic pH, and that this activation brings about an inhibition of motility in B16F10 and TRAMP-C1 tumor cells, it was next important to analyze the effects of this activation on directional migration (chemotaxis) as revealed by transwell assays. Transwell migration assays were used as a model to observe the ability for chemotaxis of the different tumor cell lines at varying pH. Cells were allowed to migrate from pH treated serum free migration media, through an 8μm-pored transwell filter, towards pH treated NIH3T3-conditioned growth media. As fibroblast cells secrete a variety of growth factors, chemokines and cytokines, and are an integral part of the extra cellular matrix, their growth media was used as a chemoattractant in the migration assay to mimic the fibroblastic tumor microenvironment. This assay allowed for the visualization and quantification of the effect of GPR4 activation on directional migration, and a significant inhibition of the ability for migration was observed upon full activation of GPR4 in different cell lines. As can be observed in Figure 3, upon overexpression and activation of GPR4 there was a significant ($p<0.05$) inhibition in the ability for directional chemotaxis in both B16F10 and TRAMP-C1 tumor cells as indicated by the number of cells that migrated through the transwell filter (3A, 3C). Images were taken of the transwell filters, with migrated cells stained purple (3B, 3C). There is a noticeable

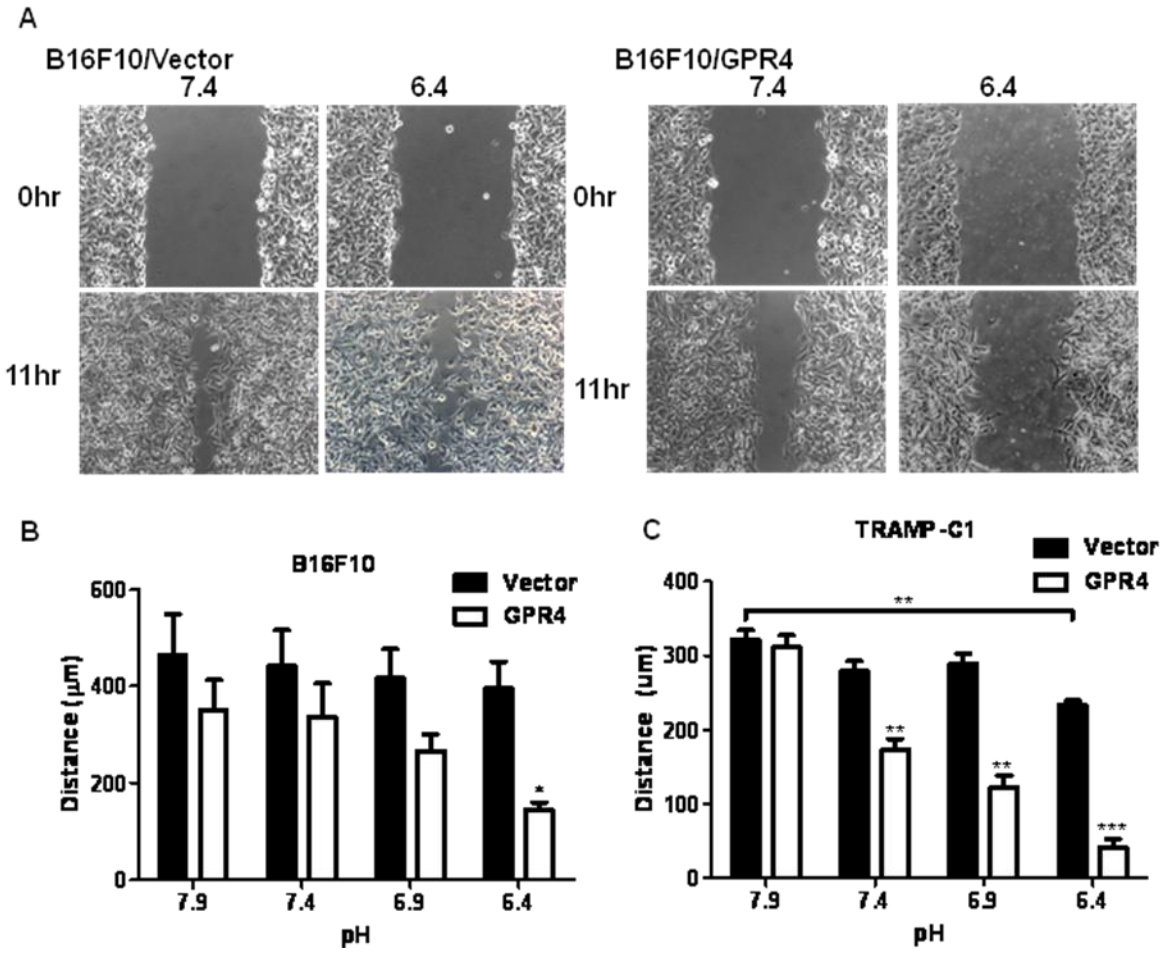

Figure 2. B16F10 and TRAMP-C1 Cell Wound Closure Assays. (A) Images of B16F10 and TRAMP-C1 wound closure. Images were taken of B16F10/Vector and B16F10/GPR4 cells at the 0 and 11 hour marks. Cells were treated with growth media pH buffered to 7.9, 7.4, 6.9 or 6.4. (B) Quantification of B16F10 wound closure. The extent of wound closure was quantified by measuring the distance cells traveled (μm) after 11 hours. These results are the average of three independent experiments. (C) Quantification of TRAMP-C1 wound closure. The extent of wound closure was quantified by measuring the distance cells traveled (μm) after 6 hours. These results are the average of three independent experiments. *P<0.05, **P<0.01, and ***P<0.001, compared to Vector cells at each pH.

inhibition of migration upon the overexpression and subsequent activation of GPR4 in the tumor cells.

GPR4 Activation Inhibits the Ability for Invasion Through the Extra Cellular Matrix

As it was deduced that GPR4 activation by acidosis inhibits both the spontaneous motility and directional migration of B16F10 and TRAMP-C1 tumor cells, it was next necessary to analyze the effect of GPR4 activation on tumor cell invasion through the extra cellular matrix (ECM). With the ability for degradation and subsequent invasion through the ECM being an integral part of tumor cell metastasis, transwell invasion assays through a layer of matrigel were performed in an attempt to mimic this process. Matrigel is designed to resemble the dense stroma and connective tissue that is characteristic of the ECM. Ice cold matrigel was applied to the top of 8μm transwell filters, and cells were allowed to migrate from pH buffered migration media, through the matrigel and transwell filter, towards pH buffered NIH3T3-conditioned media. Overexpression and activation of GPR4 by acidosis, especially at a pH of 6.4, significantly inhibited the ability for B16F10/GPR4 and TRAMP-C1/GPR4 cells to invade through the matrigel layer (Figures 4A and 4B). Figure 4 illustrates a pH dependent decrease in the invasive capability of B16F10/GPR4 and TRAMP-C1/GPR4 cells in comparison to B16F10/Vector and TRAMP-C1/Vector cells.

GPR4 Activation Decreases the Ability for Tumor Cells to Degrade Gelatin

To further elucidate the mechanism by which GPR4 activation inhibits the invasion of tumor cells through the extra cellular matrix, a gelatin degradation assay was performed with the intent to analyze how GPR4 activation affects the ability for tumor cell degradation. Degradation of the ECM is an important step in tumor cell invasion and

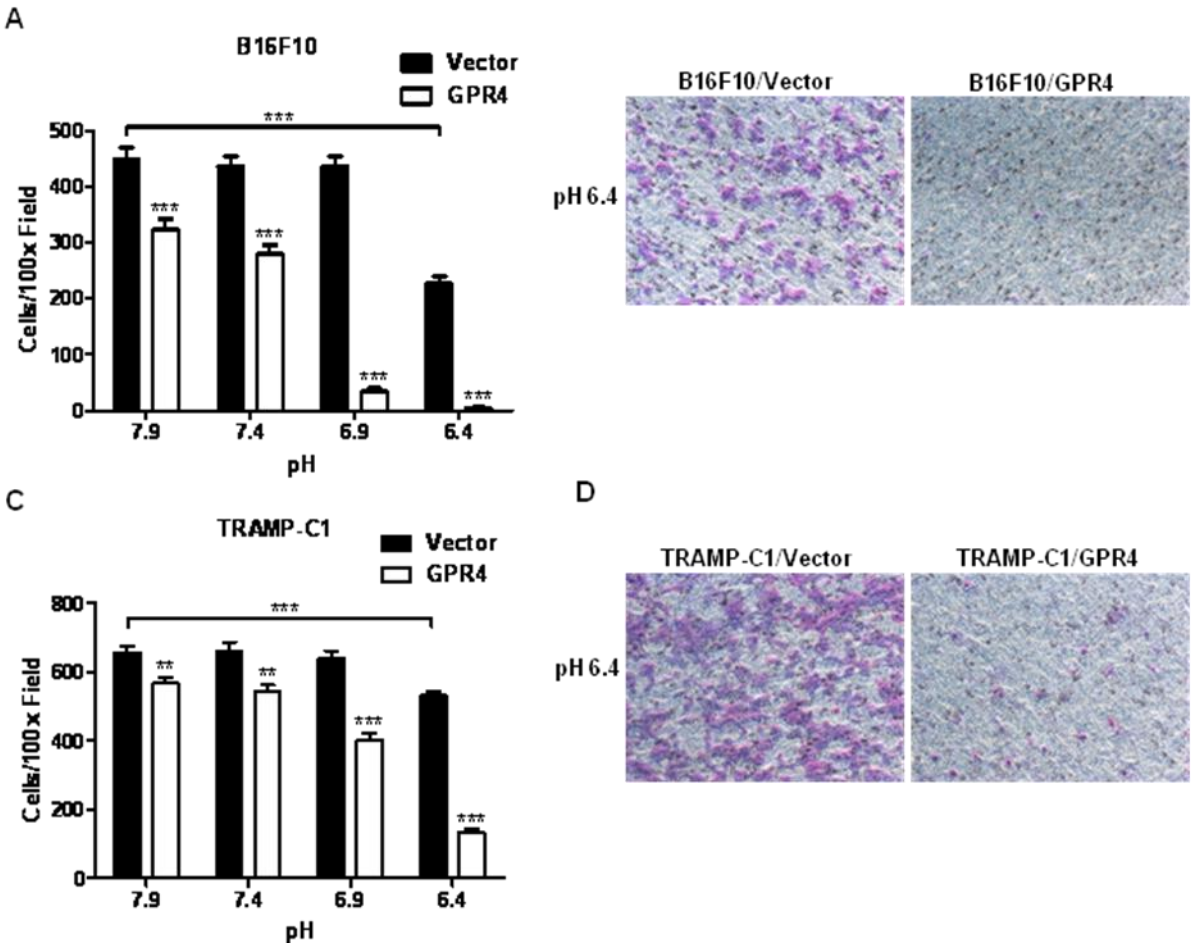

Figure 3. B16F10 and TRAMP-C1 Transwell Migration Assays. (A) B16F10 transwell migration assay at varying pH. $1x10^5$ B16F10/Vector or B16F10/GPR4 cells were allowed 6 hours to migrate from pH buffered serum free migration media, through a transwell filter with 8μm pores, to pH buffered NIH3T3 conditioned media. Migrated cells were stained with 0.2% crystal violet and counted using a 10x objective. Three fields were counted for each filter. These results are the average of three independent experiments. (B) Photos of B16F10 chemotaxis migration assay. Photos were taken of the transwell filters after the fixing and staining of migrated cells. (C) TRAMP-C1 transwell migration assay at varying pH. $1x10^5$ TRAMP-C1/Vector or TRAMP-C1/GPR4 cells were allowed 3 hours to migrate from pH buffered serum free migration media, through a transwell filter with 8μm pores, to pH buffered NIH3T3 conditioned media. Migrated cells were stained with 0.2% Crystal Violet and counted using a 10x objective. Three fields were counted for each filter. These results are the average of three independent experiments. (D) Photos of TRAMP-C1 chemotaxis migration assay. Photos were taken of the transwells after the fixing and staining of migrated cells. **P<0.01 and ***P<0.001, compared to Vector cells at each pH.

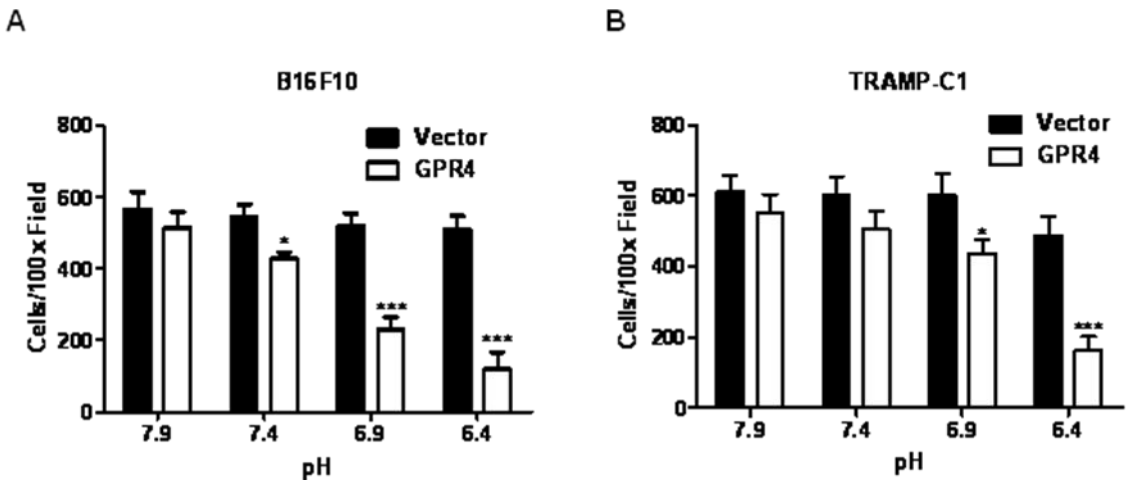

Figure 4. B16F10 and TRAMP-C1 ECM Invasion Assays. (A) B16F10 transwell ECM invasion assay at varying pH. $1x10^5$ B16F10/Vector or B16F10/GPR4 cells were resuspended in pH buffered migration media, applied to the top of a 50μL layer of a 2:1 mixture of water:matrigel, and allowed 20 hours to invade towards pH buffered NIH3T3 conditioned media. Migrated cells were stained with 0.2% crystal violet and counted using a 10x objective. Three fields were counted for each transwell filter. These results are the average of two independent experiments. (B) TRAMP-C1 transwell ECM invasion assay at varying pH. $1x10^5$ TRAMP-C1/Vector or TRAMP-C1/GPR4 cells were resuspended in pH buffered migration media, applied to the top of a 50μL layer of a 2:1 mixture of water:matrigel, and allowed 16 hours to invade towards pH buffered NIH3T3 conditioned media. Migrated cells were stained with 0.2% crystal violet and counted using a 10x objective. Three fields were counted for each transwell filter. These results are the average of two independent experiments. *P<0.05, **P<0.01 and ***P<0.001, compared to Vector cells at each pH.

metastasis as cells must first degrade their immediate environment so as to expose a niche for their invasion. Therefore, plating cells on top of fluorescently labeled gelatin and allowing them to attach and enter the cell cycle offered a means to observe degradation of the gelatin by the tumor cells, indicative of degradation of the ECM. A 0.2% gelatin and Alexa Fluor 555 conjugate was purified and confirmed via coomassie blue staining and gel electrophoresis. Analysis under white light revealed identical patterns of bands between 0.2% gelatin and the 0.2% Gelatin/Alexa Fluor 555 conjugate. The sizes of the bands of the Gelatin/Alexa Fluor 555 conjugate were slightly larger than those of gelatin only, likely due to the conjugation of the Alexa Fluor 555. As expected, under UV light, only the 0.2% Gelatin/Alexua Fluor 555 conjugate offered bands, confirming proper conjugation and purification (Figure 5A). Cell culture slides were then coated with the 0.2% Gelatin/Alexa Fluor 588 conjugate and B16F10/Vector and B16F10/GPR4 tumor cells were plated on top of the slides and allowed ample time to attach, enter the cell cycle, and degrade the conjugated gelatin. Fluorescent microscopy was used to image the degradation, and analysis was performed by determining the percentage of cells that showed conjugated gelatin degradation, and by measuring the area of degradation. It was then determined that GPR4 overexpression and activation by acidosis significantly inhibited the ability for B16F10 degradation. B16F10/GPR4 cells showed a decrease in both the number of cells exhibiting degradation and area of degradation at an acidic pH in comparison to B16F10/GPR4 cells at a pH 7.9 and B16F10/Vector cells at all pH (Figures 5B and 5C). This phenotype could be due to a decrease in the secretion of proteases by activated and overexpressed GPR4 in tumor cells. This aspect will be investigated in future studies.

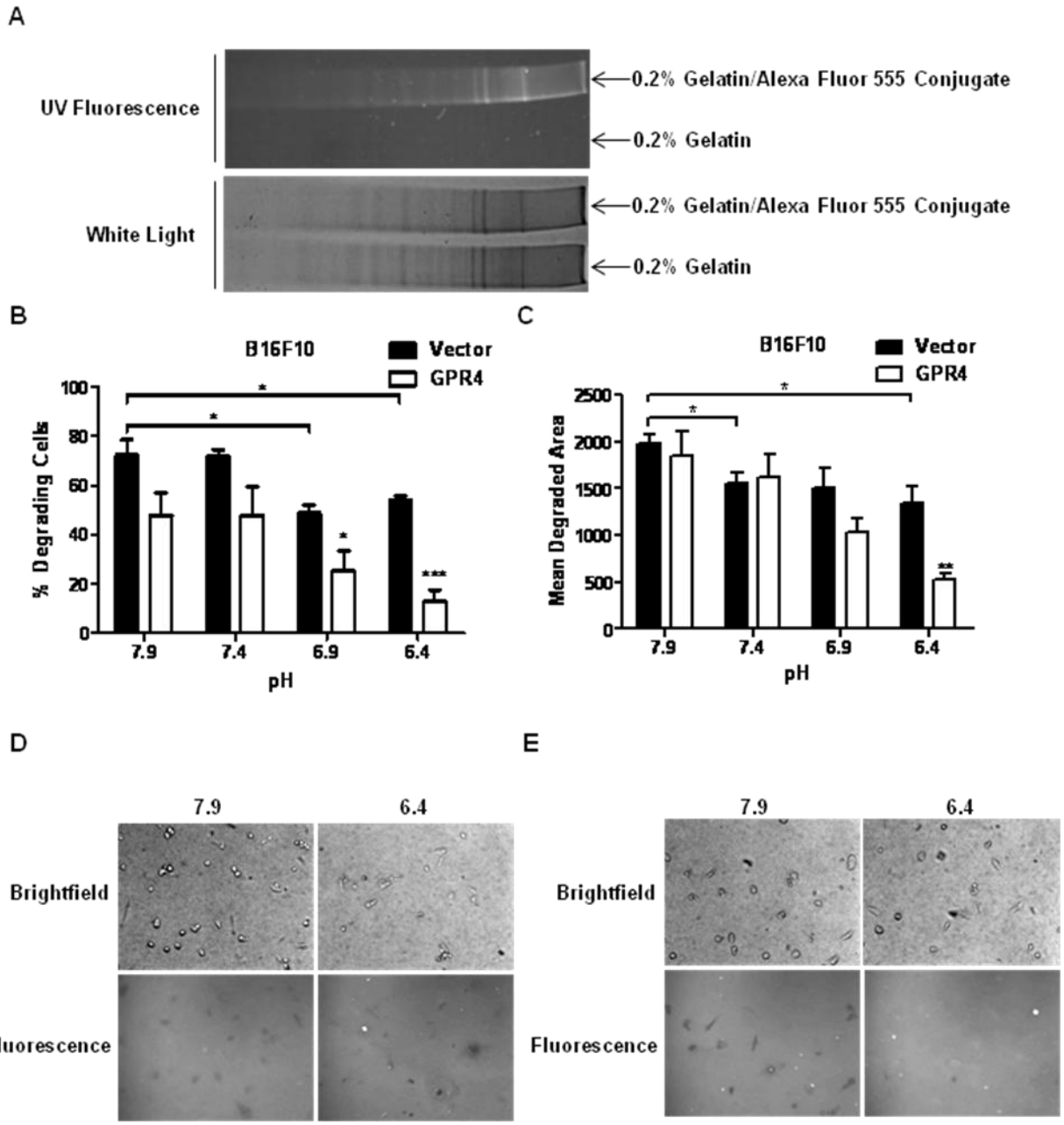

Figure 5. B16F10 Degradation Assay. (A) Gel electrophoresis of the 0.2% Gelatin/AlexaFluor 555 conjugate. 0.2% Gelatin protein was conjugated with AlexaFluor 555. 0.2% Gelatin and the conjugate were then stained and gel electrophoresis performed. Images were analyzed under both white light and UV fluorescence. (B) Percentage of B16F10 cells showing degradation. B16F10/Vector or B16F10/GPR4 cells were plated on 0.2% gelatin/AlexuaFluor 555 coated cell culture slides, treated with pH buffered growth media, and allowed 28 hours to attach and enter the cell cycle. Images were then analyzed using fluorescent microscopy and the percentage of cells showing degradation determined. (C) Average area of degraded regions. The area of degraded regions corresponding to live cells was measured using

ImageJ imaging software. (D) Images of B16F10/Vector degradation assay at varying pH. Photos of the B16F10 cells were taken through a 10x objective using both white light and fluorescence. (E) Images of B16F10/GPR4 degradation assay at varying pH. Photos of the B16F10 cells were taken through a 10x objective using both white light and fluorescence. These results are the average of four independent experiments. *$P<0.05$, **$P<0.01$ and ***$P<0.001$, compared to Vector cells at each pH.

GPR4 Activation Inhibits the Ability for Invasion through an Endothelial Cell Monolayer

To further investigate the effect of acidosis activation of GPR4 on invasion, a layer of HUVEC endothelial cells was allowed to form a confluent monolayer on the top of the transwell filters. This assay mimicked another integral step in tumor cell metastasis, the ability for cells to extravasate and intravasate through a layer of endothelial cells. As blood and lymph vessels are composed of endothelial cells, this assay resembles tumor cell invasion into and out of the blood stream. Tumor cells were allowed to migrate from pH buffered migration media, through the layer of HUVEC endothelial cells and the transwell filter, towards NIH3T3 conditioned media. As expected, the invasive ability of GPR4 overexpressing tumor cells was greatly inhibited upon overexpression and acidosis activation when compared to vector overexpressing cells of the same pH. (Figures 6A and 6B).

GPR4 Activation Increases Claudin-1 Expression in HUVEC Cells

As data indicated there was a strong inhibition in the ability of GPR4 overexpressing tumor cells to invade through a HUVEC endothelial cell monolayer at an acidic pH, it was next important to deduce a possible molecular mechanism by which HUVEC cells could contribute to the acquired phenotype. Microarray data revealed an upregulation of the integral tight junction protein Claudin-1 in GPR4 overexpressing HUVEC cells at an acidic pH, and it was thought that an upregulation in the levels of Claudin-1 by endogenous mGPR4 could result in the observed inhibitory phenotype. Figure 7 depicts western blot confirmation of this hypothesis as it was seen that upon treatment of HUVEC/Vector cells with acidosis there was a noticeable increase in Claudin-1 levels in the HUVEC/Vector cells when compared to cells treated with a basic

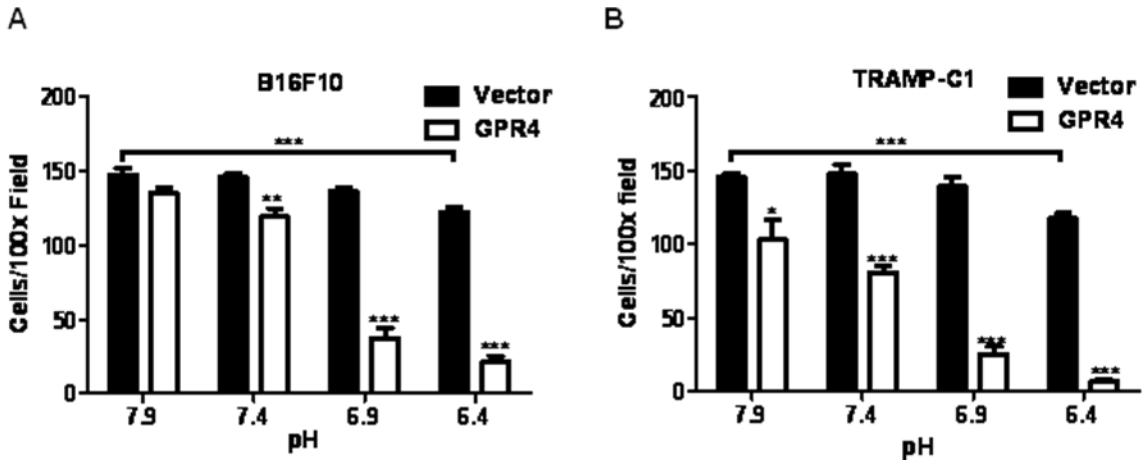

Figure 6: Tumor Cell Invasion Through a HUVEC Endothelial Cell Monolayer. (A) B16F10 invasion through a HUVEC endothelial cell monolayer. $1x10^5$ HUVEC/Vector cells were plated on top of an 8μm transwell filter and allowed 24 hours to attach and proliferate. $1x10^5$ B16F10/Vector or B16F10/GPR4 cells, resuspended in pH buffered migration media, were then applied to the top of the endothelial cell monolayer and allowed 20 hours to invade through towards pH buffered NIH3T3 conditioned media. Migrated cells were then stained and counted using a 10x objective. Three fields were counted for each transwell filter. These results are the average of two independent experiments. (B) TRAMP-C1 invasion through a HUVEC endothelial cell monolayer. $1x10^5$ HUVEC/Vector cells were plated on top of an 8μm transwell filter and allowed 24 hours to attach and proliferate. $1x10^5$ TRAMP-C1/Vector or TRAMP-C1/GPR4 cells, resuspended in pH buffered migration media, were then applied to the top of the endothelial cell monolayer and allowed 16 hours to invade through towards pH buffered NIH3T3 conditioned media. Migrated cells were then stained and counted using a 10x objective. Three fields were counted for each transwell filter. These results are the average of two independent experiments. *$P<0.05$, **$P<0.01$ and ***$P<0.001$, compared to Vector cells at each pH.

or neutral pH.

GPR4 Inhibits the Pulmonary Metastasis of B16F10 Cells

Up to this point, the phenotype of inhibited migration, invasion and motility upon acidosis activation of GPR4 has been well characterized. To continue characterizing the effects of GPR4 on tumor cell motility and metastasis, it was next important to analyze how GPR4 affects *in vivo* metastasis. A pulmonary melanoma metastasis model was adopted to observe the ability of B16F10/GPR4 cells to metastasize to a distant location in comparison to B16F10/Vector cells. Using syngeneic C57BL/6 wild type mice as our murine model, tail vein injections of the aforementioned tumor cells were performed and the occurrence of pulmonary tumor nodules analyzed. It was found that B16F10/Vector cells show a high rate of pulmonary metastasis, while B16F10/GPR4 cells showed strong inhibition of pulmonary metastasis (Figure 8A). Close to 80% inhibition of pulmonary metastasis was observed in B16F10/GPR4 cells in comparison to B16F10/Vector cells (Figure 8B).

GPR4 Overexpression Slightly Inhibits the Rate of B16F10 Primary Tumor Formation

To further investigate the *in vivo* effects of overexpressing GPR4, a subcutaneous melanoma injection assay was carried out to observe any differences in the rate of primary tumor formation between B16F10/Vector and B16F10/GPR4 cells. As opposed to observing distant metastasis, this assay offered a means to observe differences in the growth rate and final mass of primary tumors arising from the subcutaneous injection of B16F10/Vector and B16F10/GPR4 cells in a C57BL/6 murine model. A trend was observed in that the rate of primary tumor formation and subsequent final tumor mass (Figure 9A and B), was slightly inhibited upon overexpressing GPR4. This trend,

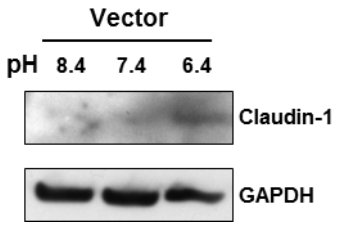

Figure 7. Western Blot Analysis of Claudin-1 Expression in HUVEC Cells at Varying pH. HUVEC/Vector cells were treated with pH buffered growth media overnight. Western blot analysis was then performed to detect Claudin-1 protein expression. This image is representative of two independent experiments.

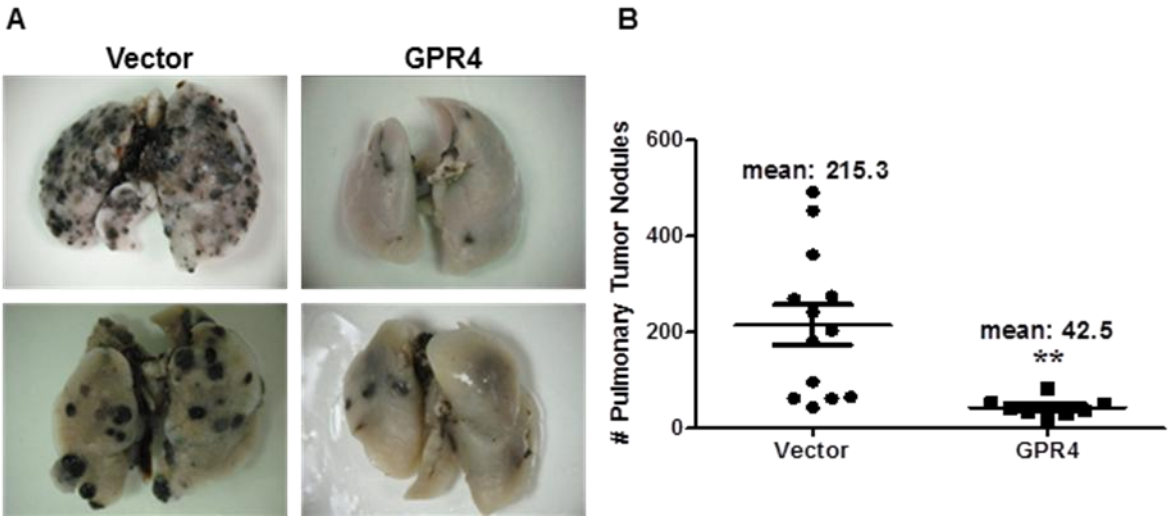

Figure 8. B16F10 Pulmonary Metastasis *in vivo* Assay. (A) Photos of lungs from pulmonary melanoma metastasis of B16F10 cells. $2x10^5$ B16F10 cells were injected intravenously through the tail vein of C57BL/6 wildtype female mice. Cells were allowed 16 days to metastasize at which point the lungs were dissected out, fixed, and pulmonary tumor nodules counted. (B) Quantitative data from the pulmonary melanoma metastasis of B16F10/Vector and B16F10/GPR4 cells assay. Thirteen mice were injected with B16F10/Vector cells, and eight mice were injected with B16F10/GPR4 cells. **P<0.01, compared to Vector cells.

however, was not statistically significant as the P value was greater than 0.05.

GPR4 Activation Slightly Reduces Cell Proliferation

With the rate of B16F10 primary tumor formation being slightly reduced upon overexpression of GPR4, it was next important to analyze differences in cell viability and proliferation. B16F10/Vector and B16F10/GPR4 cells were treated with varying pH for up to 2 days, and an MTT assay was used to quantify live cells in the culture. There was a slight, non significant inhibition of cell proliferation upon acidosis activation of overexpressed GPR4 in B16F10 cells, as indicated by the MTT ratio depicted in Figure 10.

GPR4 Activation Induces Actin Stress Fiber Formation

With both *in vitro* and *in vivo* assays indicating an inhibition of tumor cell migration and metastasis upon overexpression and activation of GPR4, it was next important to begin deducing the molecular mechanism that could contribute, at least partially, to the observed phenotype. The activation of the small GTPase Rho results in the formation of actin stress fibers, which are known to play a role in cell motility. As the OGR1 family of G protein coupled receptors, inclusive of GPR4, is known to activate the $G_{12/13}$/Rho pathway under certain stimuli, it was thought to analyze the occurrence of actin stress fiber, indicative of the pathway in question (28). Figure 11 visualizes the high occurrence of stress fiber formation upon acidosis activation of B16F10/GPR4 cells in comparison to cells treated with a basic or neutral pH. Furthermore, treatment of B16F10/GPR4 cells with CN01, a known cell permeable Rho activator, showed similarities in the rate of stress fiber formation when compared to B16F10/GPR4 cells activated by an acidic pH. Although this assay is not a direct quantification of activated

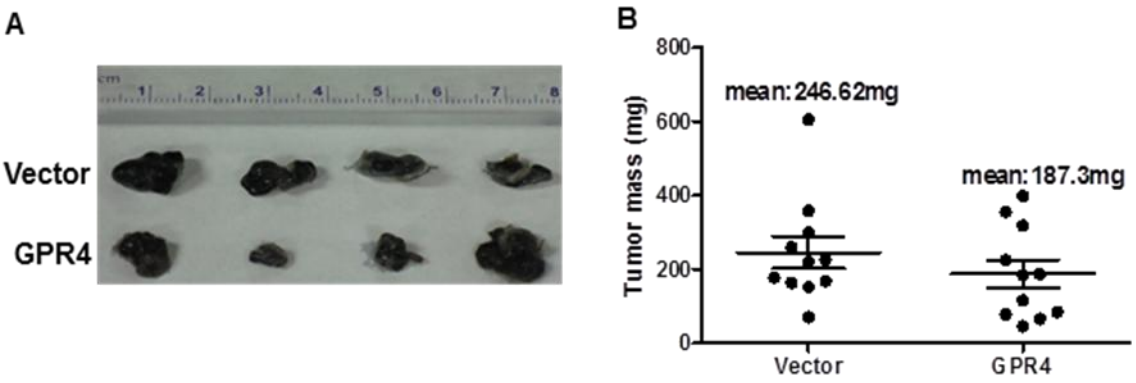

Figure 9. B16F10 Subcutaneous Melanoma Injection. (A) Photos of B16F10 subcutaneous melanoma injection. $2x10^5$ B16F10/Vector and B16F10/GPR4 cells were injected subcutaneously on the hip flank of C57BL/6 wildtype female mice. Cells were allowed 14 days to form primary tumors, with the length, width and height of the tumors being measured every four days. After 14 days the tumor were dissected and weighed. (B) Quantitative data from B16F10 subcutaneous melanoma injection. 11 mice were injected with B16F10/Vector cells, and 11 with B16F10/GPR4 cells. P=0.32.

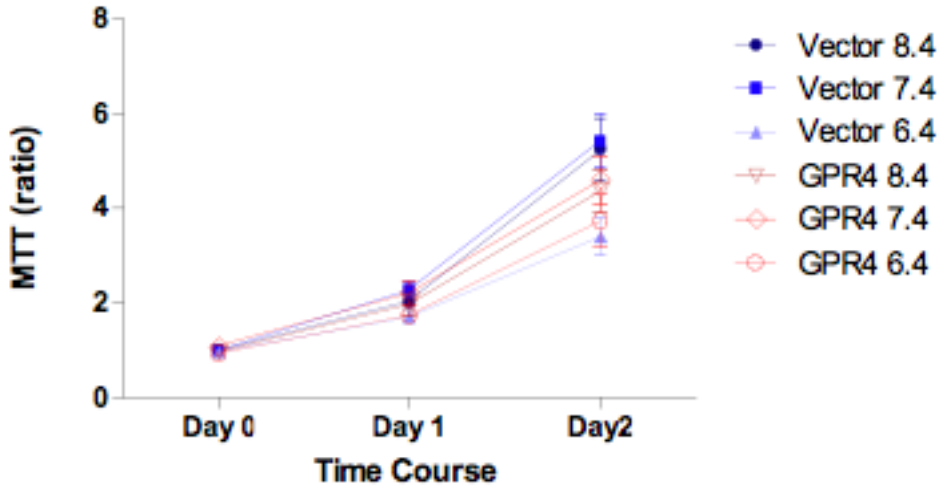

Figure 10. MTT Assay of B16F10 Cells at Varying pH. An MTT assay was performed for two days on B16F10/Vector and B16F10/GPR4 cells. This data is the average of five independent experiments.

levels of Rho, it offers an indirect means of observing how pH and CN01 may influence the levels of activated Rho as visualized through the occurrence of actin stress fibers.

CN01 Inhibits B16F10 Cell Motility

As it has been reported [28] and confirmed by actin staining (Figure 11) that GPR4 activation by acidosis increases the levels of activated RhoA, it was thought that this change in the cytoskeletal phenotype could contribute to the inhibition of motility and metastasis observed upon GPR4 activation in tumor cells. To test this hypothesis, B16F10/Vector cells were treated with the known cell permeable RhoA activator CN01 (Calpeptin) and the effect of Rho activation on directional motility observed using a wound closure assay. It was found that treatment with 0.5unit/mL CN01 inhibited the ability of B16F10/Vector cells for wound closure (Figure 12A). This phenotype was significant at all pH tested in comparison to B16F10/Vector cells treated with 2.5μL/mL of DMSO, the solvent for CN01 (Figure 12B).

CN01 Inhibits Pulmonary Metastasis of B16F10/Vector Cells

After determining that Rho activation by CN01 inhibits the ability for B16F10/Vector cells for directional motility, it was next important to determine if Rho activation affected the ability for B16F10/Vector cell pulmonary metastasis. B16F10/Vector cells were pretreated for two hours with either 0.5unit/mL CN01 or 2.5μL/mL DMSO, and $2x10^5$ tumor cells were injected in the tail vein of C57BL/6 wild type female mice and allowed 16 days to metastasize. There was significant inhibition in the rate of B16F10/Vector pulmonary metastasis after treatment of cells with CN01 when compared to cells treated with DMSO, indicating that this treatment inhibits B16F10/Vector metastasis *in vivo* (Figure 13).

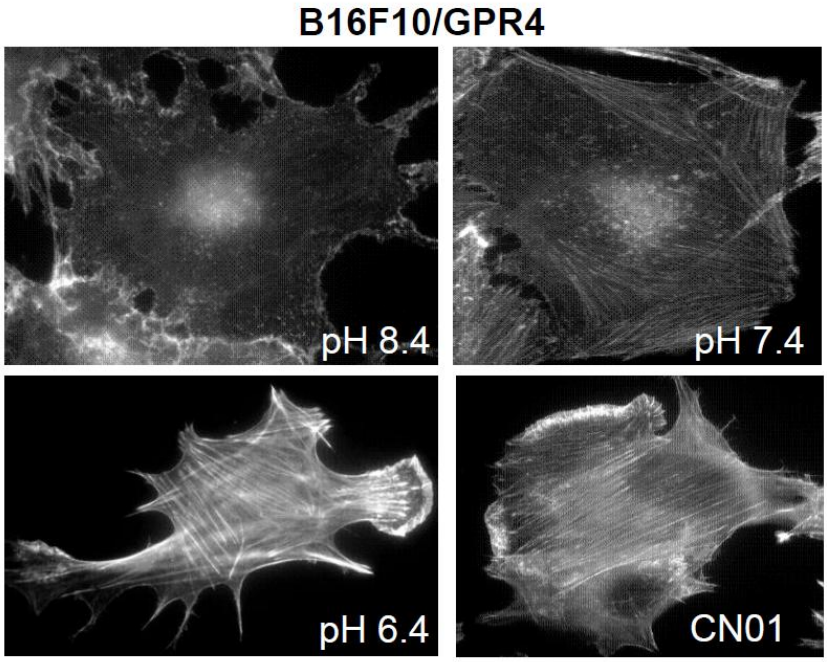

Figure 11. B16F10 Actin Staining Upon Treatment at Varying pH. B16F10 cells were serum starved for three days then treated with pH buffered serum free media or serum free media with CN01. Cells were then fixed, permealized and stained with Rhodamine Phalloidin. Pictures were then taken using a fluorescent microscope. Images are representative of three independent experiments.

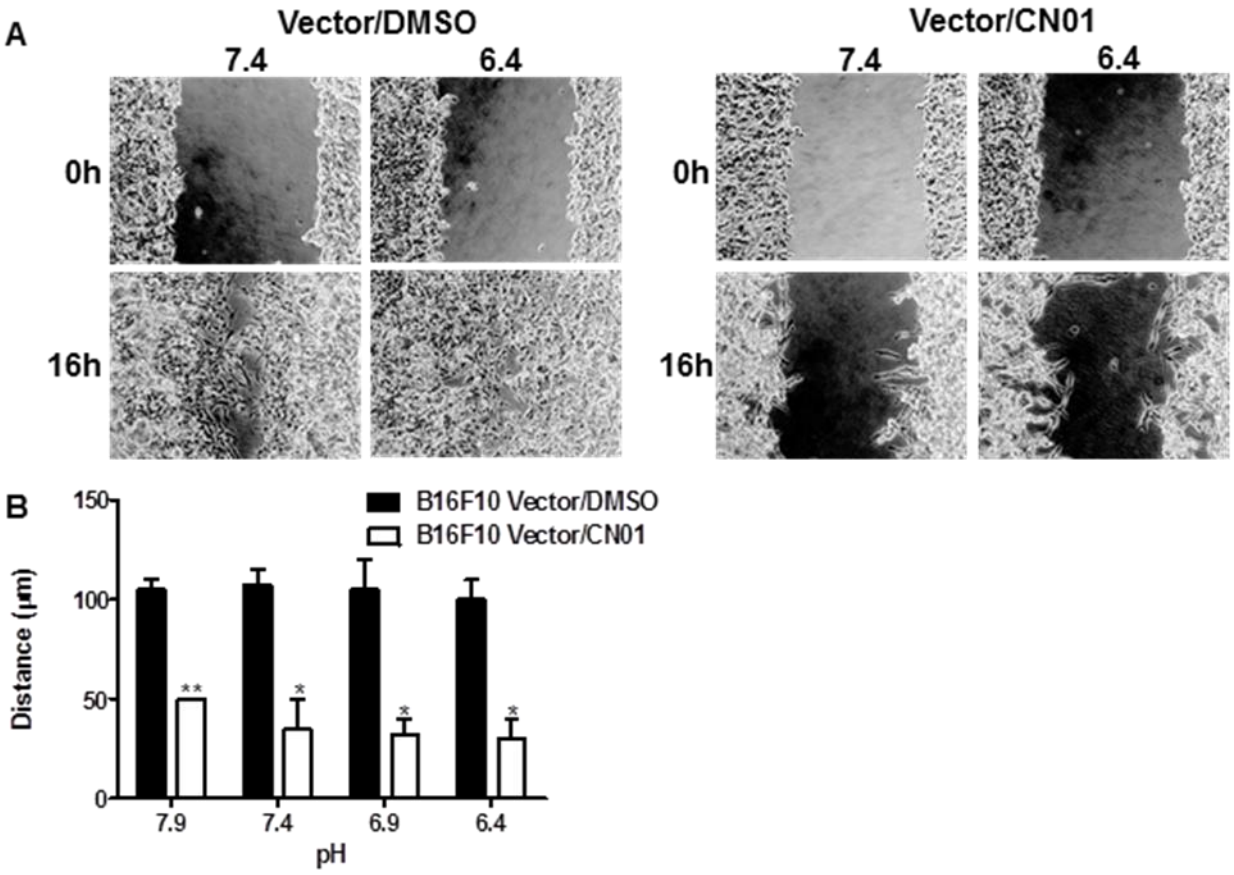

Figure 12. B16F10 Wound Closure at Varying pH and Upon Treatment with CN01. (A) Photos of B16F10/Vector cell wound closure after treatment with CN01. B16F10/Vector cells were allowed to grow to confluency at which point a wound was created and the cells treated with either 0.5unit/mL CN01 or 2.5μL/mL DMSO in growth media buffered to varying pH. Photos were taken at 0 and 16 hours. (B) Quantification of B16F10/Vector cell wound closure after treatment with CN01. The wounds were measured at 0 and 16 hours and the distance cells traveled determined. These results are the average of two independent experiments. *P<0.05, **P<0.01, in comparison to cells treated with DMSO at the same pH.

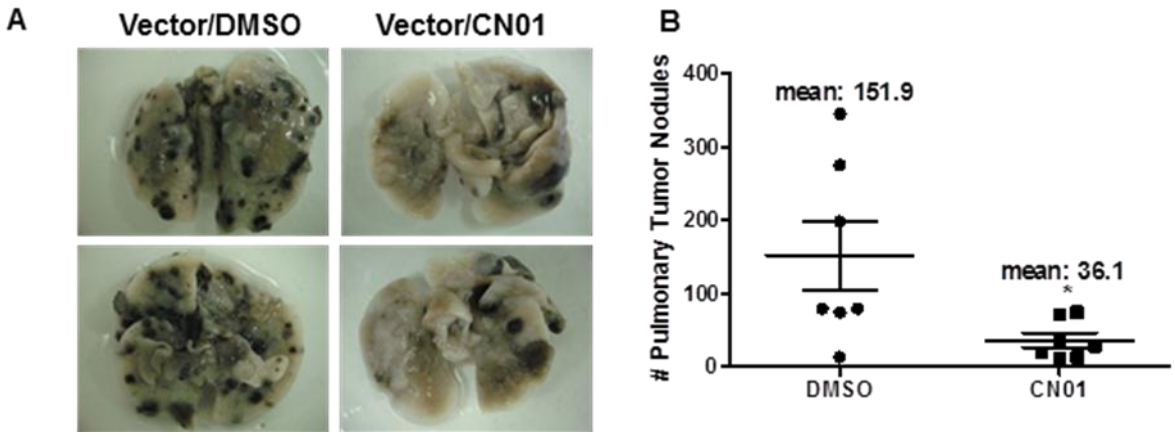

Figure 13. B16F10/Vector Pulmonary Metastasis Assay After Treatment with CN01. (A) Photos of B16F10/Vector cell pulmonary metastasis after treatment with CN01. B16F10/Vector cells were treated for two hours with either 0.5unit/mL CN01 or 2.5μL/mL DMSO in growth media. $2x10^5$ cells were then injected into female C57BL/6 wild type mice via the tail vein. Cells were allowed 16 days to metastasize at which point the lungs were dissected, fixed and analyzed. (B) Quantification of B16F10/Vector cell pulmonary metastasis after treatment with CN01. The number of pulmonary tumor nodules was counted using a dissecting microscope. Seven mice were injected with B16F10/Vector-DMSO cells, and seven with B16F10/Vector-CN01 cells. *$P<0.05$, in comparison to DMSO treated cells.

CN01 Slightly Increases the Rate of Primary Tumor Formation

To continue with the *in vivo* analysis of the effect of Rho activation on B16F10/Vector cells, a subcutaneous melanoma injection assay was utilized to determine the rate of primary tumor formation. B16F10/Vector cells treated for two hours with either 0.5unit/mL CN01 or 2.5μL/mL DMSO and $2x10^5$ cells were injected subcutaneously on the hip flank of female C57BL/6 wild type mice. It was observed that CN01 slightly increases the rate of B16F10/Vector cell primary tumor formation in comparison to cells treated with DMSO, however these results were not statistically significant (Figure 14).

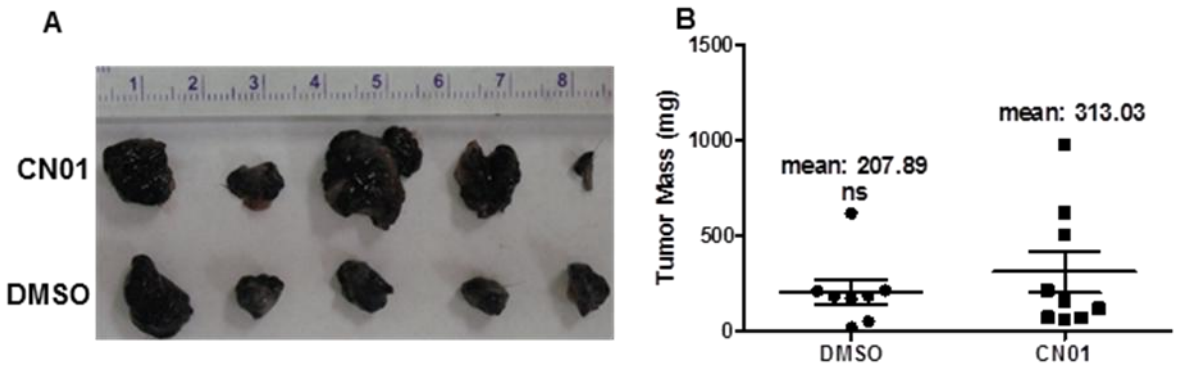

Figure 14. B16F10/Vector Subcutaneous Melanoma Injection After Treatment with CN01. (A) Primary tumors from the B16F10/Vector subcutaneous melanoma injection after treatment with CN01. $2x10^5$ B16F10/Vector and B16F10/GPR4 cells were injected subcutaneously on the hip flank of C57BL/6 female mice. Cells were allowed 14 days to form primary tumors, with the length, width and height of the tumors being measured every four days. After 14 days the tumor were dissected and weighed. (B) Primary tumors from the B16F10/Vector subcutaneous melanoma injection after treatment with CN01. Eight and nine mice were injected with B16F10/Vector cells treated with DMSO and CN01, respectively. P=0.42.

Chapter 4: Discussion

The acquisition of a motile and metastatic phenotype is one of the most devastating properties developed by many types of cancerous cells, often resulting in a severely worsened prognosis. Traditionally and historically cancer has been treated via the excision of the primary tumor by surgery or direct radiation, with this procedure adequate at eradicating localized cancerous tissue [12, 21]. However, upon metastasizing, strategies for combating the cancer become less efficient. These treatments often result in non-specific cell death and eradication, bringing about widespread tissue damage and a decrease in patient quality of life. Rather than complete eradication of cancerous tissue, the final result is often only an extension of patient survival [21, 51]. It is therefore of the upmost importance to develop novel strategies to combat cancer metastasis. Drugs and therapies designed to prevent the initial acquisition of an invasive phenotype would greatly increase the life expectancy and prognosis of many types of cancer. As cell metastasis is a very complex and involved process, there exists the potential for numerous opportunities to inhibit the ability for cells to metastasize. From an inability to detach from the primary tumor, to a decrease in viability in the lymph and vascular systems or inhibition of the ability to arrest, extravasate and colonize, the beneficial implications of strategically targeting the pathways involved in metastasis are blatant and widespread.

Recent years have seen the tumor microenvironment present numerous novel targets for the development of new cancer fighting strategies. From cell autonomous to inclusive of the tumor microenvironment, the current view of cancer not only incorporates the cancerous cells found within the primary tumor, but also the various

cells, tissues and factors present in the immediate environment that help dictate tumor progression [3]. It is now known that the tumor microenvironment can influence many different aspects of the progression of the cancer, inclusive of its ability for metastasis [12]. Many characteristics of the tumor microenvironment present evolutionary constraints on tumor cells. Tumor cells resistant to certain harsh microenvironmental conditions are often left with a highly invasive and progressive phenotype, as Darwinian evolution dictates a model of survival of the fittest [12, 17]. The hallmarks of the tumor microenvironment that have been found to actively select for advanced tumor cells are hypoxia, acidosis and high interstitial fluid pressure [14, 17].

Acidosis is a well-defined characteristic of the tumor microenvironment. Thought to arise due to alterations in metabolism and glycolysis, acidosis not only selects for invasive and progressive cancer cells, but also induces cell death in neighboring, non-tumorigenic cells, in turn facilitating the tumor cell's expansion and invasion into the newly created niche [19, 20, 23]. These conditions make microenvironmental acidosis an interesting topic of research. A potential for drug discovery lies in development of means to combat the ability for tumor cells to exist in a viable and tumorigenic state within microenvironmental acidosis. Furthermore, it is possible to capitalize on the existence of acidosis by delineating molecular pathways which inhibit the ability of tumor cells for proliferation and metastasis in response to acidosis.

The incredible diversity of the GPCR family of receptors leaves them as the target for the majority of therapeutic agents [25, 28]. As the largest family of cell surface receptors, GPCRs are responsible for directing an array of cellular functions, from endocrine activity, to immune responses, to regulating cell proliferation [24, 25].

Furthermore, GPCRs are found in a large number of tumor cells, implicating a function in certain processes of tumorigenesis [27]. Their function in tumorigenesis, however, is not well defined. Recently, a family of proton sensing G-protein coupled receptors has been identified that are activated by extracellular protons [29, 30]. As microenvironmental acidosis is due to the accumulation of extracellular protons, this family of receptors, and their subsequent downstream pathways, may be the target for novel and realistic therapeutic strategies.

GPR4, a member of the aforementioned family of proton sensing GPCRs, has been shown to be fully activated at an acidic pH. Furthermore, this activation results in the initiation of numerous signaling pathways, some of which may be directly involved in cell motility and metastasis. Specifically, acidosis activation of GPR4 induces activation of the $G_{12/13}$/Rho signalling pathway, a pathway responsible for actin reorganization, an important process in cell motility [29, 30, 46]. Activation of the $G_{12/13}$/Rho pathway by GPCRs has been shown to result in an inhibition of cell motility and migration in some cell systems [36, 47]. Furthermore, GPR4 has been shown to couple to the G_s pathway, which results in the activation of the cAMP pathway. Exchange proteins activated by cAMP (EPAC) overexpression has been shown to increase the invasive ability of melanoma cells, implying that the G_s pathway, like the $G_{12/13}$, may play a roll in migration and invasion [52]. cAMP/PKA signaling is also reported to influence cell migration and cytoskeletal rearrangement as some important steps in cell motility and metastasis, like Cdc42 and Rac activation, require the influence of the cAMP/PKA signaling pathway [53]. The G_q pathway has also been reported to play a role in motility regulation [47]. Although the activation of GPR4 by acidosis has been well defined,

there exists very little indication of how the activation will influence the ability for tumor cells to acquire a motile and metastatic phenotype. With GPR4 activation having been previously reported to activate signaling pathways directly involved in cell motility, and G-protein coupled receptors being the target of the majority of therapeutics, GPR4 provides an excellent target for the development of novel anti-cancer therapies.

B16F10 melanoma and TRAMP-C1 prostate cancer cells offer a good model for the characterization of the effect of GPR4 overexpression and activation on tumor cell motility and metastasis. As both cell types express low levels of endogenous mouse GPR4 (Figure 1), the overexpression of huGPR4 should clearly highlight the effects, if any, of GPR4 activation on cellular processes. In fact, overexpression of huGPR4 was successful in both B16F10 and TRAMP-C1 cell lines, as can be observed in Figure 1. As both B16F10 and TRAMP-C1 cell lines are highly motile, overexpression of huGPR4 left us with a working model in which to analyze the effects of GPR4 activation on tumor cell motility.

In concordance with previous results, our series of *in vitro* cell motility (Figure 2), migration (Figure 3) and invasion (Figures 4 and 6) assays, along with our actin stress fiber assay (Figure 12), confirmed that GPR4 is fully activated at an acidic pH [29]. While this data clearly highlights that GPR4 is activated at an acidic pH, it also confers that GPR4 activation has an effect on tumor cell motility. We observed that overexpression and full activation of GPR4 at an acidic pH results in a strong inhibition of cell motility. Furthermore, it appears that acidosis activation of GPR4 increases the occurrence of actin stress fibers, indicating an upregulation of activated GTP bound Rho as facilitated by the $G_{12/13}$/Rho signaling pathway. Although the formation of actin stress

fibers is indicative of Rho activation, actin stress fiber staining only offers an indirect means of analyzing the levels of activated Rho.

Figure 2 depicts the results of numerous wound closure assays performed on B16F10 and TRAMP-C1 cells. Wound closure assays are used to analyze differences in directional, spontaneous motility, and it was seen that GPR4 overexpression and activation inhibits the ability for tumor cells to close the wound. As GPR4 activation upregulates the Rho pathway, it was thought to treat vector overexpressing B16F10 cells with CN01, a chemical containing the known cell permeable Rho activator calpeptin. In fact, treatment with CN01 inhibited the ability for B16F10/Vector cells to close the wound (Figure 13), indicating that Rho activation may be responsible for the phenotype of motility inhibition.

Previous studies have shown that a delicate regulation of Rho activation is critical for cell migration. In some cases, studies have indicated that an increase in the levels of Rho-GTP actually increase cell motility and metastasis [44]. Others, however, have reported that upregulation of Rho-GTP acts to inhibit cell motility [36, 47]. It seems the most plausible explanation for the contradictory results is the necessity for tight regulation in the levels of activated Rho, as steps and processes involved in motility require an upregulation of Rho-GTP, and others a downregulation.

Mesenchymal motility, defined by elongated and polarized cell morphology, is characteristic of B16F10 cells [45]. This form of motility requires differing levels of Rho at different stages in the process [45]. During mesenchymal motility, Rac1 and Cdc42, members of the Rho family of GTPases, are responsible for cell polarization and directionality, respectively. RhoA and its effecter ROCK, however, need to be reduced

to extend protrusions at the front of the cell [36, 39, 45]. This is a crucial step in mesenchymal motility as it enables the formation of new, focal adhesion complexes, along with the subsequent "pulling" of the cell forward [36, 39]. Furthermore, Rho is involved in the occurrence of focal adhesion complexes, as its activation is needed to form them, and its inactivation necessary for the process of focal adhesion turnover, which propels the cell forward [36, 46]. These facts, therefore, could account for the observed motility inhibition of the highly motile B16F10/Vector cells upon treatment with CN01 (Figure 12). By constituently activating Rho, CN01 may induce the occurrence of focal adhesion complexes, inhibit protrusions at the leading edge of the cell, and decrease the ability for focal adhesion turnover. These effects would certainly culminate in the observed inhibition of motility found upon CN01 activation of Rho in B16F10/Vector cells.

We further characterized the effects of GPR4 activation on tumor cell motility by examining chemotaxis as revealed by transwell assays. Chemotaxis is a form of directional migration in which cells respond to different chemokines and signals to migrate along a chemical gradient. By isolating NIH3T3 cell-conditioned media, we were able to mimic an aspect of the tumor microenvironment as fibroblasts are found in the connective tissue and extra cellular matrix surrounding the tumor [12]. Therefore, by applying it to the bottom of a transwell migration chamber, we were able to analyze how cells responded to the chemical gradient created between the migration media and the NIH3T3 chemoattractant. It was seen that B16F10 and TRAMP-C1 cells responded well to the factors secreted by the NIH3T3 fibroblasts as this chemoattractant induced high levels of directional migration in B16F10 and TRAMP-C1 vector overexpressing cells, as

well as GPR4 overexpressing tumor cells at a basic pH. However, upon full activation of GPR4 by acidosis, there was a significant inhibition of the GPR4 overexpressing tumor cells to migrate towards the chemoattractant. Therefore, GPR4 overexpression and subsequent activation not only inhibit the motility of tumor cells, but also their ability to respond to and migrate towards a chemoattractant (Figure 3).

Invasion through the extra cellular matrix is an import step in the initiation of tumor cell metastasis. This process requires the degradation of the extra cellular matrix, often by matrix metalloproteinases, and the subsequent movement of the tumor cell through this newly vacant space. Matrigel is used to resemble the ECM *in vitro*, with the ability for cells to invade through it being indicative of their ability to move through the actual ECM. We found that GPR4 overexpression and activation greatly reduced the ability for B16F10 and TRAMP-C1 tumor cells to invade through matrigel, and thus the ECM (Figure 4). The observed phenotype of motility inhibition upon GPR4 activation could be due to an arrest of cells in the ECM, a decrease in the motility of cells through the ECM, a decrease in the cells ability to respond to the chemoattractant, decrease in the ability of the tumor cells to degrade the ECM, or a combination of any and all of these contributors. It was in fact found that GPR4 activation and overexpression inhibited the ability of B16F10 cells to degrade gelatin (Figure 5). Although we report that activation of GPR4 by acidosis inhibits the ability for degradation of the extra cellular matrix, other studies have indicated that specific microenvironmental conditions increase the invasiveness of tumor cells. Hypoxia has been reported to increase the secretion of matrix metalloproteinases (MMP-2 and MMP-9) in pancreatic, colorectal and breast tumor cells, a characteristic that could be attributed to hypoxia induced acidosis [54].

Moellering *et al.* reported that acidosis treatment of melanoma cells resulted in the acquisition of a more invasive and motile phenotype, with other reports indicating the same phenotype and attributing it to change in gelatinase activity [55, 56]. However, this phenotype was clearly not replicated in our B16F10/Vector and B16F10/GPR4 cell lines using the gelatin degradation assay, and this trend could be attributed to differences between tumor cell lines or different assays. It has been shown that different members of the MMP family can exhibit different and contradictory roles in tumor cell progression, with individual MMPs often contradicting their own function at different stages in tumor cell progression. Overall, however, MT1-MMP, MMP-2 and MMP-9 have been reported to be proteolytic activating, resulting in the degradation of immediate physical barriers and subsequent migration and invasion [57]. Therefore, it is possible that GPR4 activation results in a decrease of pro-invasive MMPs. The observed inability for activated GPR4 overexpressing tumor cells to degrade the ECM may play a role in the observed inhibition of invasion, with this phenotype potentially being due to a reduction in specific MMPs. The potential role of GPR4 in regulating protease expression or activity warrants further investigation. Although in many aspects acidosis, and the subsequent evolution of tumor cells to resist acidosis, increases the invasive and metastatic phenotype of tumor cells, it is possible that GPR4, with its unique ability to respond to and become activated by extracellular protons, presents a novel means to inhibit metastasis and invasion in response to acidosis.

As intravasation and extravasation through endothelial cells is a crucial aspect in the ability of cells to metastasize, we analyzed the influence, if any, GPR4 overexpression and activation had on the ability for tumor cells to invade through a

HUVEC endothelial cell monolayer. This assay is important as it highlights a step of metastasis that enables tumor cells to travel through the blood stream and colonize in distant locations. As expected, GPR4 activation in tumor cells reduced their ability to invade through the endothelial cell monolayer (Figure 6). The culmination of huGPR4 activation in tumor cells and possible endogenous mGPR4 activation in endothelial cells resulted in a very strong inhibition of invasion. This phenotype could arise due to the fact that GPR4 activation activates the GTPase Rho, whose activation is correlated with an increase in focal adhesion complexes. Therefore, tumor cells overexpressing activated GPR4 may bind very strongly with the endothelial cells found in the monolayer, especially if GPR4 activation in endothelial cells causes an increase in cell-cell cadherins. Furthermore, analysis of microarray data indicated that acidosis activation of GPR4 in HUVEC cells increased the expression of Claudin-1, a tight junction protein. With this data confirmed by western blot analysis (Figure 7), it is possible that Claudin-1 could contribute to the observed phenotype of motility inhibition, with an increase in tight junctions decreasing the permeability of the endothelial cell monolayer.

After fully characterizing the effects of acidosis activation of GPR4 on *in vitro* tumor cell motility, migration and invasion, it was necessary to utilize *in vivo* models for examining metastasis and primary tumor formation. Using tail vein injections on mice, it was found that GPR4 overexpression greatly reduced the pulmonary metastasis of B16F10 cells (Figure 8). This phenotype is the culmination of those observed during the *in vitro* assays, with *in vivo* metastasis incorporating many of the mechanisms tested *in vitro*, from migration, to invasion through the extra cellular matrix, to invasion through an endothelial cell monolayer. It must be noted, however, that cells were not treated with

an acidic pH prior to injection. Therefore, it appears the physiological pH sufficiently activates GPR4 to result in the metastasis inhibitory phenotype. Although full activation of GPR4 is found between a pH of 6.8-6.4, reports have indicated significant activation between a pH of 7.4 and 7.0, and we have seen a decrease in *in vitro* motility and migration at a physiological pH. It therefore appears the lower levels of activation found at a physiological pH is sufficient at inhibiting the *in vivo* metastasis of GPR4 overexpressing B16F10 cells. As it is thought that Rho is involved in the observed inhibition of motility upon acidosis activation of GPR4 *in vitro*, we hypothesized that activating Rho in the highly metastatic B16F10/Vector cells would decrease their ability for pulmonary metastasis. This hypothesis was confirmed as pretreating B16F10/Vector cells with CN01 prior to injection greatly reduced the cell's ability for metastasis (Figure 13). As previously stated, Rho activation increases cell-cell adhesion, so it is possible cells became arrested in the mouse vasculature before being able to colonize in the lungs. Constitutive activation of Rho also decreases the ability for cells to extend protrusions which results in an inhibition of mesenchymal motility, another potential explanation for the observed phenotype *in vivo*.

Although GPR4 overexpression resulted in a profound effect on *in vivo* tumor cell metastasis, it resulted in no significant difference between the rate of *in vivo* B16F10 primary tumor formation or *in vitro* B16F10 cell proliferation (Figures 9 and 10, respectively). While there is a noticeable trend of GPR4 overexpression slightly decreasing the rate of primary tumor formation, this result is not statistically significant and it is consistent with those results obtained with the MTT assay. Furthermore, Rho activation by CN01 seems to slightly increase the rate of primary tumor formation of

B16F10/Vector cells in comparison to those treated with DMSO as a control (Figure 14). This observation, however, is not statistically significant, and could be attributed to an increase in adhesion and interaction with the extra cellular matrix and surrounding cells. Rho proteins are involved in a variety of tumorogenic processes, inclusive of cell cycle progression, an evasion of apopotisis, cytoskeletal rearrangement, interaction with surrounding fibroblasts, and degradation of the ECM [58]. Therefore, if Rho activation stimulates adhesion and interactions within the extra cellular matrix, it is possible that B16F10/Vector cells will have an increased ability for primary tumor formation after treatment with CN01.

The results characterized in this thesis have important implications in tumor cell biology. These results offer a novel means of inhibiting tumor cell motility and metastasis, that being through activation of GPR4 by acidosis or small molecules. This is an exciting finding as GPCRs are widely used as therapeutic targets. In terms of developing therapeutic applications from these findings, a potential lies in the development of an agonist that successfully and fully activates endogenous levels of GPR4 in human primary tumors, in turn offering a means of inhibiting the acquisition of a metastatic phenotype. Furthermore, upon fully deducing the molecular mechanisms by which GPR4 inhibits motility and metastasis, it may be possible to develop a drug which utilizes the same mechanisms to prevent metastasis in human patients. Future directions for this project include the full characterization of the molecular pathway responsible for the observed inhibition of motility and migration. In addition to determining the exact mechanism by which the activation of Rho seemingly plays a part in the observed motility and metastasis inhibition, it will be important to characterize differences in the

occurrence of focal adhesion complexes, the rate of focal adhesion turnover, trends in the epithelial-mesenchymal transition between different cell types, and differences in the secretion of proteases responsible for extra cellular matrix degradation. Although there is much to be learned in the future, the findings in this thesis present a strong starting point towards the development of a novel anti-metastasis therapy that capitalizes on the observed effects of motility and metastasis inhibition upon overexpression and acidosis activation of GPR4.

References

1. Jemal, A., et al., *Cancer statistics, 2010.* CA Cancer J Clin. **60**(5): p. 277-300.
2. Jemal, A., et al., *Cancer statistics, 2009.* CA Cancer J Clin, 2009. **59**(4): p. 225-49.
3. Hanahan, D. and R.A. Weinberg, *The hallmarks of cancer.* Cell, 2000. **100**(1): p. 57-70.
4. *Cancer Facts & Figures 2010.* American Cancer Society, 2010.
5. Barth, A., L.A. Wanek, and D.L. Morton, *Prognostic factors in 1,521 melanoma patients with distant metastases.* J Am Coll Surg, 1995. **181**(3): p. 193-201.
6. Middleton, M.R., et al., *Randomized phase III study of temozolomide versus dacarbazine in the treatment of patients with advanced metastatic malignant melanoma.* J Clin Oncol, 2000. **18**(1): p. 158-66.
7. Tawbi, H.A. and S.C. Buch, *Chemotherapy resistance abrogation in metastatic melanoma.* Clin Adv Hematol Oncol. **8**(4): p. 259-66.
8. Hoeflich, K.P., et al., *Oncogenic BRAF is required for tumor growth and maintenance in melanoma models.* Cancer Res, 2006. **66**(2): p. 999-1006.
9. Flaherty, K.T., *Narrative review: BRAF opens the door for therapeutic advances in melanoma.* Ann Intern Med. **153**(9): p. 587-91.
10. Held, L., et al., *Oncogenetics of melanoma: basis for molecular diagnostics and therapy.* J Dtsch Dermatol Ges.
11. Guise, T., *Examining the metastatic niche: targeting the microenvironment.* Semin Oncol. **37 Suppl 2**: p. S2-14.
12. Lorusso, G. and C. Ruegg, *The tumor microenvironment and its contribution to tumor evolution toward metastasis.* Histochem Cell Biol, 2008. **130**(6): p. 1091-103.
13. Hanahan, D. and R.A. Weinberg, *Hallmarks of cancer: the next generation.* Cell. **144**(5): p. 646-74.
14. Fukumura, D. and R.K. Jain, *Tumor microenvironment abnormalities: causes, consequences, and strategies to normalize.* J Cell Biochem, 2007. **101**(4): p. 937-49.
15. Balkwill, F. and A. Mantovani, *Inflammation and cancer: back to Virchow?* Lancet, 2001. **357**(9255): p. 539-45.
16. Cairns, R., I. Papandreou, and N. Denko, *Overcoming physiologic barriers to cancer treatment by molecularly targeting the tumor microenvironment.* Mol Cancer Res, 2006. **4**(2): p. 61-70.
17. Gatenby, R.A. and R.J. Gillies, *A microenvironmental model of carcinogenesis.* Nat Rev Cancer, 2008. **8**(1): p. 56-61.
18. Gatenby, R.A. and R.J. Gillies, *Glycolysis in cancer: a potential target for therapy.* Int J Biochem Cell Biol, 2007. **39**(7-8): p. 1358-66.
19. Gatenby, R.A. and R.J. Gillies, *Why do cancers have high aerobic glycolysis?* Nat Rev Cancer, 2004. **4**(11): p. 891-9.
20. Pedersen, P.L., *Warburg, me and Hexokinase 2: Multiple discoveries of key molecular events underlying one of cancers' most common phenotypes, the "Warburg Effect", i.e., elevated glycolysis in the presence of oxygen.* J Bioenerg Biomembr, 2007. **39**(3): p. 211-22.

21. Steeg, P.S., *Tumor metastasis: mechanistic insights and clinical challenges.* Nat Med, 2006. **12**(8): p. 895-904.
22. Vander Heiden, M.G., L.C. Cantley, and C.B. Thompson, *Understanding the Warburg effect: the metabolic requirements of cell proliferation.* Science, 2009. **324**(5930): p. 1029-33.
23. Gatenby, R.A., et al., *Acid-mediated tumor invasion: a multidisciplinary study.* Cancer Res, 2006. **66**(10): p. 5216-23.
24. Yang, L.V., et al., *Vascular abnormalities in mice deficient for the G protein-coupled receptor GPR4 that functions as a pH sensor.* Mol Cell Biol, 2007. **27**(4): p. 1334-47.
25. Sin, W.C., et al., *G protein-coupled receptors GPR4 and TDAG8 are oncogenic and overexpressed in human cancers.* Oncogene, 2004. **23**(37): p. 6299-303.
26. Lee, H.J., B. Wall, and S. Chen, *G-protein-coupled receptors and melanoma.* Pigment Cell Melanoma Res, 2008. **21**(4): p. 415-28.
27. Lundstrom, K., *Latest development in drug discovery on G protein-coupled receptors.* Curr Protein Pept Sci, 2006. **7**(5): p. 465-70.
28. Lappano, R. and M. Maggiolini, *G protein-coupled receptors: novel targets for drug discovery in cancer.* Nat Rev Drug Discov. **10**(1): p. 47-60.
29. Ludwig, M.G., et al., *Proton-sensing G-protein-coupled receptors.* Nature, 2003. **425**(6953): p. 93-8.
30. Singh, L.S., et al., *Ovarian cancer G protein-coupled receptor 1, a new metastasis suppressor gene in prostate cancer.* J Natl Cancer Inst, 2007. **99**(17): p. 1313-27.
31. Mahadevan, M.S., et al., *Isolation of a novel G protein-coupled receptor (GPR4) localized to chromosome 19q13.3.* Genomics, 1995. **30**(1): p. 84-8.
32. Tomura, H., et al., *Proton-sensing and lysolipid-sensitive G-protein-coupled receptors: a novel type of multi-functional receptors.* Cell Signal, 2005. **17**(12): p. 1466-76.
33. Tobo, M., et al., *Previously postulated "ligand-independent" signaling of GPR4 is mediated through proton-sensing mechanisms.* Cell Signal, 2007. **19**(8): p. 1745-53.
34. Liu, J.P., et al., *Each one of certain histidine residues in G-protein-coupled receptor GPR4 is critical for extracellular proton-induced stimulation of multiple G-protein-signaling pathways.* Pharmacol Res. **61**(6): p. 499-505.
35. Sahai, E., *Illuminating the metastatic process.* Nat Rev Cancer, 2007. **7**(10): p. 737-49.
36. Vial, E., E. Sahai, and C.J. Marshall, *ERK-MAPK signaling coordinately regulates activity of Rac1 and RhoA for tumor cell motility.* Cancer Cell, 2003. **4**(1): p. 67-79.
37. Yilmaz, M. and G. Christofori, *Mechanisms of motility in metastasizing cells.* Mol Cancer Res. **8**(5): p. 629-42.
38. Joyce, J.A. and J.W. Pollard, *Microenvironmental regulation of metastasis.* Nat Rev Cancer, 2009. **9**(4): p. 239-52.
39. Parri, M. and P. Chiarugi, *Rac and Rho GTPases in cancer cell motility control.* Cell Commun Signal. **8**: p. 23.

40. Lauffenburger, D.A. and A.F. Horwitz, *Cell migration: a physically integrated molecular process.* Cell, 1996. **84**(3): p. 359-69.
41. Friedl, P. and K. Wolf, *Plasticity of cell migration: a multiscale tuning model.* J Cell Biol. **188**(1): p. 11-9.
42. Lammermann, T. and M. Sixt, *Mechanical modes of 'amoeboid' cell migration.* Curr Opin Cell Biol, 2009. **21**(5): p. 636-44.
43. Wolf, K., et al., *Compensation mechanism in tumor cell migration: mesenchymal-amoeboid transition after blocking of pericellular proteolysis.* J Cell Biol, 2003. **160**(2): p. 267-77.
44. Ying, H., et al., *The Rho kinase inhibitor fasudil inhibits tumor progression in human and rat tumor models.* Mol Cancer Ther, 2006. **5**(9): p. 2158-64.
45. Parri, M., et al., *EphA2 reexpression prompts invasion of melanoma cells shifting from mesenchymal to amoeboid-like motility style.* Cancer Res, 2009. **69**(5): p. 2072-81.
46. Sahai, E. and C.J. Marshall, *Differing modes of tumour cell invasion have distinct requirements for Rho/ROCK signalling and extracellular proteolysis.* Nat Cell Biol, 2003. **5**(8): p. 711-9.
47. Takashima, S., et al., *G12/13 and Gq mediate S1P2-induced inhibition of Rac and migration in vascular smooth muscle in a manner dependent on Rho but not Rho kinase.* Cardiovasc Res, 2008. **79**(4): p. 689-97.
48. Sugimoto, N., et al., *Inhibitory and stimulatory regulation of Rac and cell motility by the G12/13-Rho and Gi pathways integrated downstream of a single G protein-coupled sphingosine-1-phosphate receptor isoform.* Mol Cell Biol, 2003. **23**(5): p. 1534-45.
49. Yang, L.V., et al., *Gi-independent macrophage chemotaxis to lysophosphatidylcholine via the immunoregulatory GPCR G2A.* Blood, 2005. **105**(3): p. 1127-34.
50. Overwijk, W.W. and N.P. Restifo, *B16 as a mouse model for human melanoma.* Curr Protoc Immunol, 2001. **Chapter 20**: p. Unit 20 1.
51. Pavet, V., et al., *Towards novel paradigms for cancer therapy.* Oncogene. **30**(1): p. 1-20.
52. Baljinnyam, E., et al., *Epac increases melanoma cell migration by a heparan sulfate-related mechanism.* Am J Physiol Cell Physiol, 2009. **297**(4): p. C802-13.
53. Howe, A.K., *Regulation of actin-based cell migration by cAMP/PKA.* Biochim Biophys Acta, 2004. **1692**(2-3): p. 159-74.
54. Ridgway, P.F., et al., *Hypoxia augments gelatinase activity in a variety of adenocarcinomas in vitro.* J Surg Res, 2005. **124**(2): p. 180-6.
55. Moellering, R.E., et al., *Acid treatment of melanoma cells selects for invasive phenotypes.* Clin Exp Metastasis, 2008. **25**(4): p. 411-25.
56. Martinez-Zaguilan, R., et al., *Acidic pH enhances the invasive behavior of human melanoma cells.* Clin Exp Metastasis, 1996. **14**(2): p. 176-86.
57. Gialeli, C., A.D. Theocharis, and N.K. Karamanos, *Roles of matrix metalloproteinases in cancer progression and their pharmacological targeting.* FEBS J. **278**(1): p. 16-27.
58. Sahai, E. and C.J. Marshall, *RHO-GTPases and cancer.* Nat Rev Cancer, 2002. **2**(2): p. 133-42.